Turkish Journal of Earth Sciences (Turkish J. Earth Sci.), **Vol. 16**, 2007, pp. 441–470. *Copyright ©TÜBİTAK*

Tectonic Evolution of the Kiraz Basin, Küçük Menderes Graben: Evidence for Compression/Uplift-related Basin Formation Overprinted by Extensional Tectonics in West Anatolia

TAHİR EMRE & HASAN SÖZBİLİR

Dokuz Eylül Üniversitesi, Jeoloji Mühendisliği Bölümü, Tınaztepe Yerleşkesi, Buca, TR–35160 İzmir, Turkey
(E- mail: tahir.emre@deu.edu.tr)

Abstract: The Kiraz Basin which is located at the eastern end of the Küçük Menderes Graben was previously considered to be an extensional basin. However, the data presented here allow us to infer that the tectonic evolution of the Kiraz Basin could be explained by an alternate model which suggests compression/uplift-related basin formation at the early stage of basin evolution followed, later, by block faulting in an extensional neotectonic regime. The successive compressional and extensional strain is accommodated by a predominantly NE-trending strike-slip fault system. The new model is based on the detailed mapping, field-cross sections and kinematic analyses of the studied faults. The new model requires a revision of the current regional approaches to the tectonic setting of the west Anatolian basins.

The Kiraz Basin is filled by two contrasting sedimentary packages. The older one (the uppermost Middle Miocene–Upper Miocene Suludere Formation) is developed in relation to N–S-trending compressional tectonics and uplift along the northern margin of the basin, which is controlled by reverse and strike-slip faults. During this stage, the main sedimentary trough was located along the northern margin where metamorphic rocks of the Menderes Massif and Middle Miocene andesitic volcanism (Başova andesites) form the basement. The basal unconformity with the basement rocks has been tilted to vertical, even if overturned, thus recording the uplift linked to the activity along the margin-bounding reverse/thrust fault. The Miocene strata are nearly horizontal over most of their extent and highly deformed only along the northern margin of the basin where syntectonic activity is recorded by the development of intraformational unconformities. Following the Late Miocene, thrusting of Menderes Massif rocks onto the Miocene sediments indicates that the compressional regime was active after the sedimentation of the Suludere Formation. The development of the Plio–Pleistocene Aydoğdu Formation, under the control of the Suludere and Halıköy faults that bound the Kiraz Basin to the north and south, demonstrates that the extensional tectonic regime initiated the second stage sedimentation within the Kiraz Basin. This phase corresponds to a widening of the basin in N–S direction, a process which continues up to the present.

On the basis of kinematic data collected from faults observed in the Kiraz Basin, four deformation phases have been recognized: (i) D_1 and D_2 deformations indicate north- and south-directed tectonic transport that pre-date the formation of the Kiraz Basin; (ii) D_3 deformation, reflecting syn- to post-sedimentary tectonics, is represented by intraformational unconformities and related reverse faulting; (iii) D_4 deformation gave rise to normal faults that cut and displace early structures and shapes the Kiraz basin's present-day configuration.

It is therefore proposed here that the Kiraz Basin evolved in response to two discrete stages of tectonic activity: an early phase of latest Middle Miocene–Late Miocene reverse and strike-slip faulting along only the northern margin and a later phase of Plio–Pleistocene to Recent normal faulting affecting the margins of the basin.

Key Words: Küçük Menderes Graben, Kiraz Basin, syn-compressional sedimentation, extensional tectonics, W Anatolia

Kiraz Havzası'nın Tektonik Evrimi, Küçük Menderes Grabeni: Batı Anadolu'da Genişleme Tektoniği ile Üzerlenmiş Sıkışma/Yükselmeyle İlişkili Havza Oluşumu

Özet: Küçük Menderes Grabeni'nin doğu ucunda yer alan Kiraz Havzası önceki çalışmalarda genişlemeli bir havza modeliyle açıklanmaktaydı. Ayrıntılı jeolojik haritalama ve faylardan elde edilen kinematik verilere dayanarak önerilen yeni modele göre, havza oluşumunda etkili olan sıkışma/yükselme evresini, genişlemeli Yenitektonik rejimin blok faylanma evresi izler. Bu sıkışma ve genişlemeye ait gerilim KD–GB uzanımlı doğrultu atımlı fay sistemiyle karşılanır. Batı Anadolu havzalarının tektonik evrimiyle ilgili görüşlerin, önerilen yeni model ışığında gözden geçirilmesi gerekmektedir.

Kiraz Havzası faklı özellikteki iki ana tortul paketle doldurulmuştur. Yaşlı paket (en üst Orta Miyosen–Geç Miyosen yaşlı Suludere Formasyonu) sıkışma/yükselmeyle denetlenen havzada, kuzey kenardaki yükselme ve K–G

doğrultulu sıkışma kuvvetleriyle ilişkili olarak gelişmiştir. Bu evrede, Menderes Masifi metamorfitleri ve Orta Miyosen yaşlı andezitik volkanitlerin (Başova Andezitleri) oluşturduğu temel üzerinde açınan tortul havzanın ekseni kuzey kenar boyunca yer almaktaydı. Bu tortullardaki formasyon içi uyumsuzluklar tektonikle eş yaşlı tortullaşmanın yansıması olarak kendini gösterir. Çoğu yerde düşük eğim açılı olan Miyosen tortulları havzanın kuzey kenarı boyunca yoğun bir deformasyona uğramıştır. Geç Miyosen'i izleyen evrede, sıkışma/yükselme sonucu, Miyosen tortulları havzanın kuzey kenarı boyunca havza merkezine doğru eğimlenir ve giderek düşey, hatta devrik konum kazanır. Miyosen tortullarının devrik konum kazandığı kesimlerde Menderes Masifi'nin Miyosen tortulları üzerine bindirmesi, Suludere Formasyonu'na ait tortullaşmanın sona ermesinden sonra da sıkışma tektoniğinin varlığını kanıtlar. Kiraz Havzası'nı kuzeyden ve güneyden sınırlayan Suludere ve Halıköy faylarının denetiminde gelişen Pliyo–Pleyistosen yaşlı Aydoğdu Formasyonu, genişlemeli tektonik rejiminin başladığını belgeler. Bu evre havzanın K–D doğrultusunda günümüze kadar genişlemesine katkıda bulunmaktadır.

Kiraz Havzası'ndaki fayların kinematik verileri ışığında, dört deformasyon fazı tanımlanmıştır: (i) kuzeye ve güneye doğru tektonik taşınma veren D_1 ve D_2 deformasyon fazları Kiraz Havzası'nın oluşumu öncesinde gelişmiştir. (ii) D_3 deformasyon fazı havzanın ilk evresindeki tortullaşmayla eşyaşlı ve tortullaşma sonrası tektonikle ilişkilidir ve formasyon-içi uyumsuzluklar ve ters faylarla kendini gösterir. (iii) D_4 deformasyonu yaşlı yapıları kesen ve günümüzdeki Kiraz Havzası'nı şekillendiren normal fayların gelişmesini sağlamıştır.

Sonuç olarak, bu çalışmada Kiraz Havzası'nın iki aşamada evrimleştiği önerilmektedir; Geç Orta Miyosen–Geç Miyosen dönemindeki ilk evrede, sıkışma/yükselmeye bağlı, ters ve doğrultu atımlı faylar havzanın sadece kuzey kenarında kendini gösterirken, Pliyo–Pleyistosen'den günümüze kadar süren genişlemeli tektonik rejim havzanın karşıt kenarlarında oluşan normal fay sistemiyle simgelemektedir.

Anahtar Sözcükler: Küçük Menderes Grabeni, Kiraz Havzası, sıkışmayla eşyaşlı tortullaşma, gerilmeli tektonik, Batı Anadolu

Introduction

In recent years, most of the studies done in southwestern Anatolia have been concerned with neotectonic structural elements (e.g., Arpat & Bingöl 1969; Dumont *et al.* 1979; Le Pichon & Angelier 1979, 1981; Angelier *et al.* 1981; Koçyiğit 1984; Şengör *et al.* 1985; Sözbilir & Emre 1990; Emre 1996a, b; Seyitoğlu & Scott 1991, 1992, 1996; Hetzel *et al.* 1995a, b; Emre & Sözbilir 1995; Temiz *et al.* 1998; Koçyiğit *et al.* 1999; Sarıca 2000; Yılmaz *et al.* 2000; Gessner *et al.* 2001; Işık & Tekeli 2001; Lips *et al.* 2001; Bozkurt 2001a, 2002, 2003, 2004; Sözbilir 2001, 2002; Seyitoğlu *et al.* 2002; Işık *et al.* 2003, 2004; Kaya *et al.* 2004, 2007; Purvis & Robertson 2004, 2005; Bozkurt & Rojay 2005; Erkül *et al.* 2005a, b, 2006; Rojay *et al.* 2005; Tokçaer *et al.* 2005; Bozkurt & Sözbilir 2004, 2006; Aldanmaz 2006; Ersoy & Helvacı 2007; Çiftçi & Bozkurt 2007 and references therein).

However, there are a plethora of views concerning the origin and age of extension and related graben formation that produced the present-day appearance of the region: Extension in western Anatolia has been attributed to several tectonic causes, including (1) '*tectonic escape*' model: basin formation began when – in the Late Serravalian – N–S-directed extensional forces gave rise to westward escape ('tectonic escape') of the part of Anatolia that lay between the dextral North Anatolian and sinistral East Anatolian fault zones (Dewey & Şengör 1979; Şengör 1979, 1987; Şengör & Yılmaz 1981; Şengör *et al.* 1985; Görür *et al.* 1995); (2) '*back-arc spreading*' model: back-arc extension caused by the south-southwestward migration of the Aegean trench system (McKenzie 1972); (3) '*orogenic collapse*' model: lateral spreading of the over-thickening crust following the latest Palaeogene collision across Neotethys during the latest Oligocene and lasted until the present day (Seyitoğlu & Scott 1991, 1992; Seyitoğlu *et al.* 1992); (4) '*two stage basin formation*' model: the Early Miocene extension commenced along low-angle normal faults during orogenic collapse, followed by a period of rifting controlled by high-angle normal faults in the Plio–Quaternary, separated by an interviewing short-term compression (Koçyiğit *et al.* 1999). The second period continues at present under the influence of the North Anatolian Fault Zone (Sözbilir & Emre 1996; Koçyiğit *et al.* 1999; Bozkurt 2000, 2001a, b, 2003; Bozkurt & Sözbilir 2004, 2006; Bozkurt & Rojay 2005); and (5) a recent model of Doglioni *et al.* (2002) proposes velocity differences between the overriding Aegean and Anatolian plates on the structurally underlying African Plate.

Many workers accept the interpretation that the E–W-trending Küçük Menderes valley, like the Gediz and Büyük Menderes, developed in relation to N–S extensional

tectonics as one of many E–W- to WNW–ESE-oriented grabens (e.g., Gökten *et al.* 2001; Bozkurt & Rojay 2005; Rojay *et al.* 2005 and references therein). An obvious north-dipping fault has been traced along the western half of the southern margin of the Küçük Menderes valley (Erinç 1955; Şengör *et al.* 1985); it has been noted that this fault, at its western end, passes southeast of the ancient city of Ephesus to the Aegean Sea (Dumont *et al.* 1979; Angelier *et al.* 1981). According to Rojay *et al.* (2005), the Küçük Menderes Graben has developed along an E–W-trending syncline between Beydağ-Gökçen-Tire-Belevi. Since the Miocene, there has been counter-clockwise rotation as well as three stages of deformation in the region. In the first stage, a strike-slip regime developed as a result of N–S compression; this deformation was followed by a WSW–ENE-oriented extensional regime with a strike-slip component, which in turn was succeeded by the current NW–SE- and NE–SW-oriented extensional regime, expressed at present as seismicity (Rojay *et al.* 2005). At Kiraz, Dağkızılca and Selçuk, secondary basins with varying orientations occur as extensions of the main graben and are filled by Neogene–Quaternary clastics. According to Bozkurt & Rojay (2005) there is a N–S-trending compressional phase between the older low-angle normal fault generation and the younger phase of high-angle normal faults.

In this paper, field evidence concerning the relationships of the Neogene–Quaternary rocks of the Kiraz Basin, situated at the eastern end of the Küçük Menderes Graben (Figure 1), and the tectonic evolution of the basin will be presented. The stratigraphy, facies characteristics and age of the sedimentary fill of the Kiraz Basin (Emre *et al.* 2006), and the petrographic, geochemical and geochronological characteristics of the Neogene volcanic rocks (Başova andesites) of the region (Emre & Sözbilir 2005) germane to this study will be summarized from published reports. Detailed field mapping and structural studies carried out in the study area, allow as to derive a new evolutionary structural model for the area.

The Kiraz Basin

The Kiraz Basin is located at the eastern end of the Küçük Menderes Graben (Figure 1). The basin is a minimum of 20 km long and more than 10 km wide, and its Neogene to Quaternary sediment pile exceeds 400 m in thickness. The basin displays an 'S'-shaped structural pattern being bounded from the north by NW–SE-trending and south-facing high-angle normal faults, and from the south by NW–SE-trending and north-facing normal faults (Figure 2).

Stratigrapy

The stratigraphy of the Kiraz Basin is based on the recently published paper of Emre *et al.* (2006). According to those authors, the basin fill units, formally distinguished, are divided into two formations: the Suludere and Aydoğdu formations (Figure 3). These units rest unconformably on the pre-basin fill units (e.g., metamorphic rocks of the Menderes Massif and Başova andesites). All the units will be briefly described below.

Pre-basin Fill Units

The Menderes Massif itself is bordered by the İzmir-Ankara Zone in the north, and by the Lycian Nappes in the south (Şengör & Yılmaz 1981, see Figure 1). The metamorphic rocks of the Menderes Massif predominantly exposed on the northern (Bozdağ Mountain) and southern (Aydın Mountain) shoulders of the Kiraz Basin form the footwall rocks of the Gediz detachment fault and Büyük Menderes detachment fault, respectively (Figure 1). Predominant foliation of the metamorphic rocks down to the south on the southern flank of the Bozdağ Mountain and down to the north in the northern flank of the Aydın Mountain shows synform-like structural depression (Figures 2, 3 & 4).

The Menderes Masif in the Bozdağ Mountain includes metamorphic rocks of predominantly Palaeozoic age that have been intruded by Miocene granites (Hetzel *et al.* 1995a, b; Hetzel *et al.* 1998; Koçyiğit *et al.* 1999; Yılmaz *et al.* 2000; Candan *et al.* 2001; Sözbilir 2001, 2002; Okay & Satır 2000; Şengün *et al.* 2006). The structural top of the Bozdağ Mountain is marked by the Gediz detachment fault which characteristically defines dome-and-basin structural topography (Sözbilir 2001). This fault was named by Emre (1996a, b) and by Koçyiğit *et al.* (1999) as the 'Karadut detachment fault' and the 'Çamköy detachment fault', respectively. The term 'Gediz detachment fault' was introduced by Lips *et al.* (2001) to refer to the master detachment under which the Menderes metamorphic core complex was exhumed (see

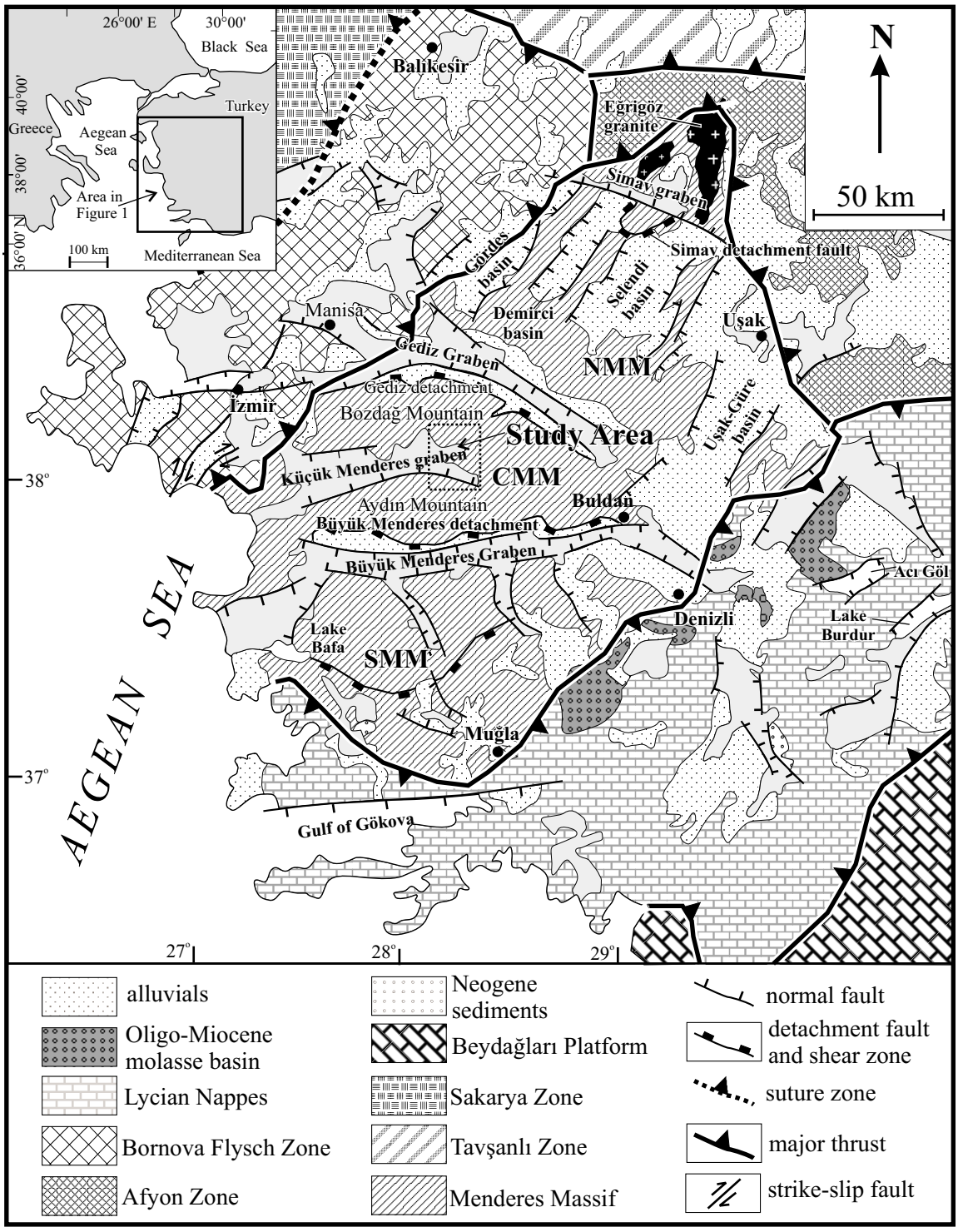

Figure 1. Regional tectonostratigraphic map of western Anatolia showing location of the study area (modified from Sözbilir 2005) NMM, CMM, SMM, IAZ are referred to northern Menderes Massif, central Menderes Massif, southern Menderes Massif and İzmir-Ankara suture, respectively.

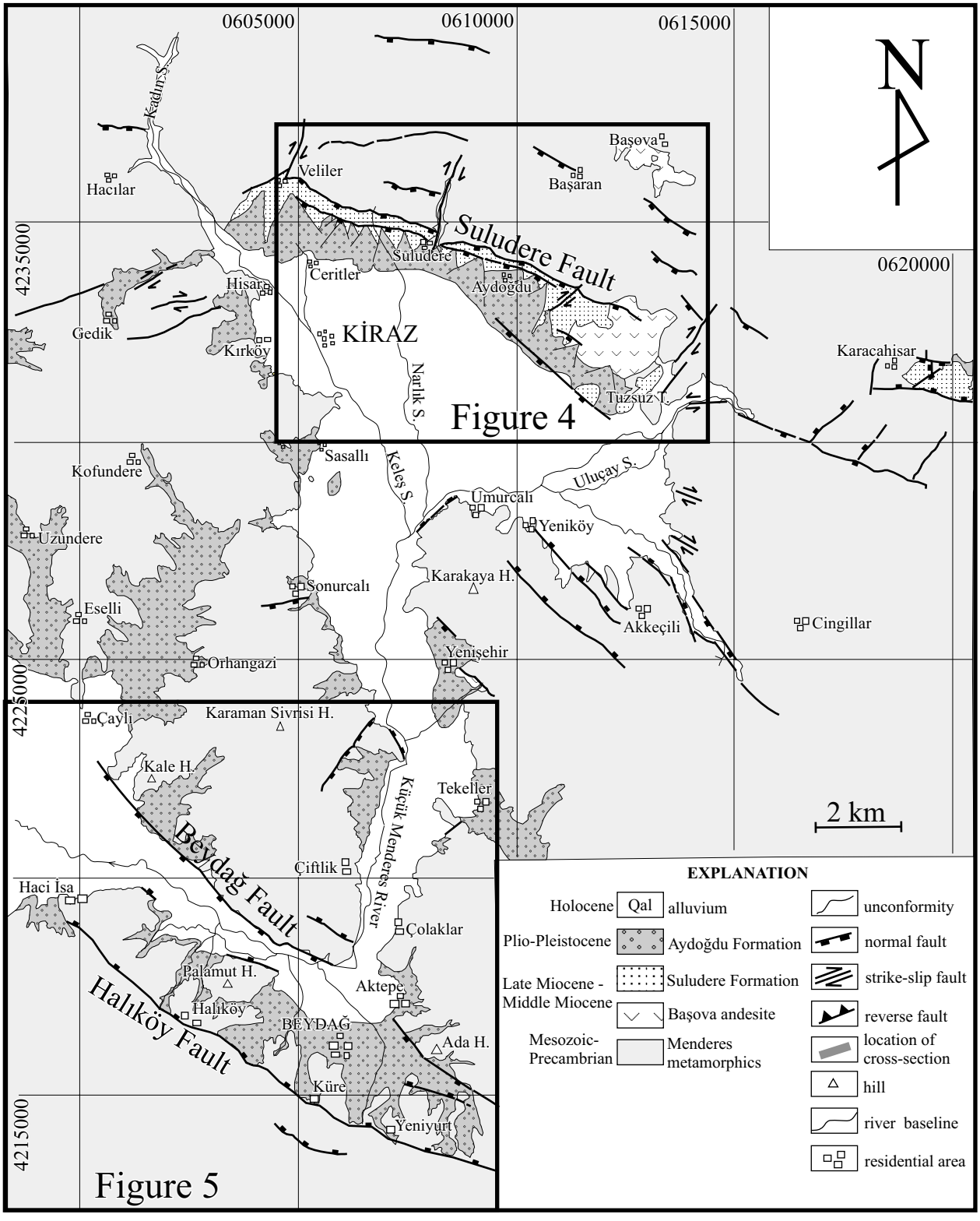

Figure 2. Simplified geological map of the Kiraz Basin (see Figure 1 for location).

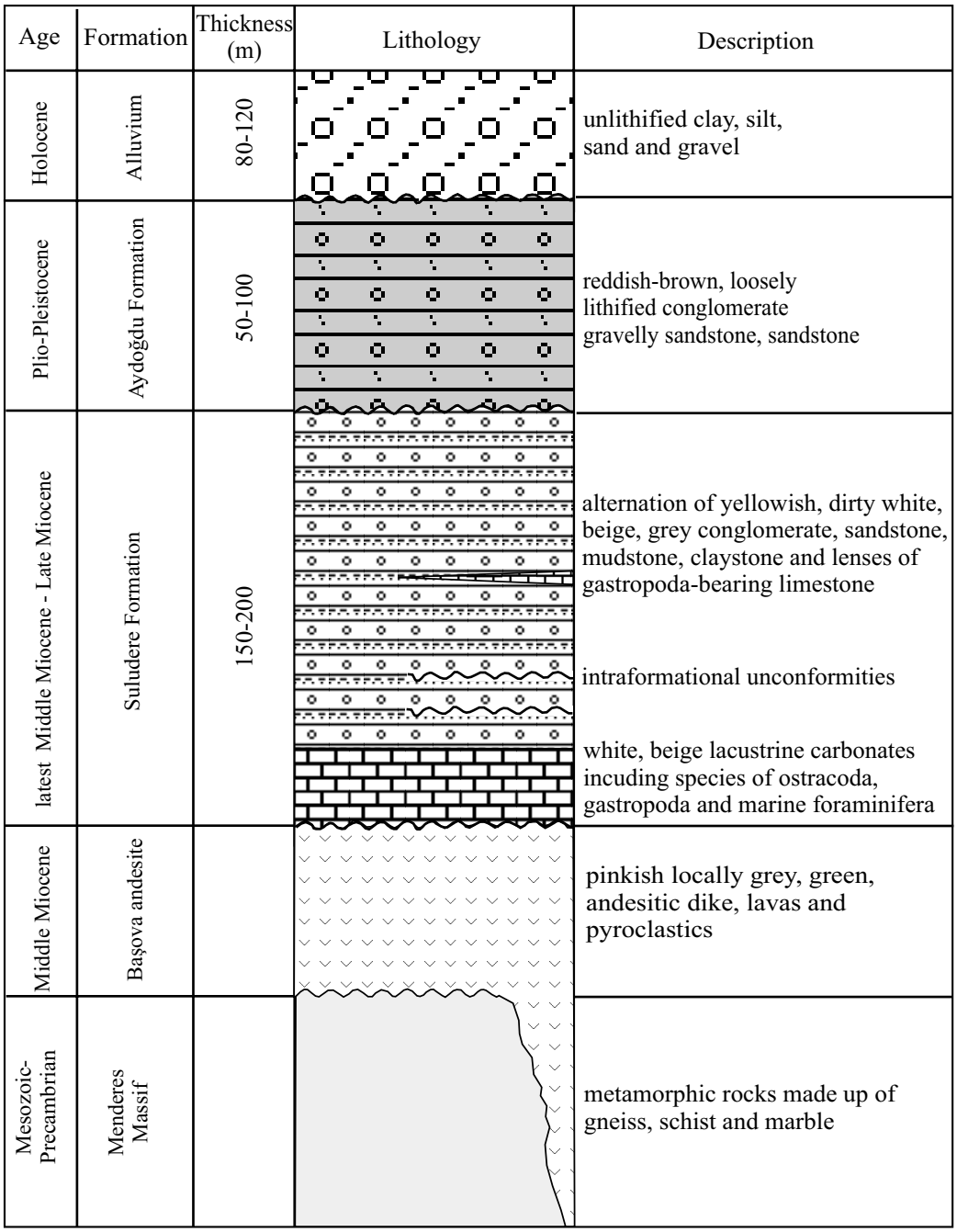

Figure 3. Lithostratigraphic columnar section of the study area (modified after Emre *et al.* 2006).

Bozkurt & Oberhansli 2001 for detail discussion of the Menderes Massif). A recent study reported by Glodny & Hetzel (2007) shows that crystallization ages of two intrusions in the footwall of the Gediz detachment fault yielded U-Pb age of 16.1±0.2 Ma (monazite, Turgutlu granodiorite) and 15.0±0.3 Ma (allanite, Salihli granodiorite). This age indicates that incipient detachment-related extensional faulting in the central Menderes Massif may be temporarily close to granotoid intrusion and thus Early to Middle Miocene (Late Burdigalian) in age. This is consistent with the age of the Başova Andesite that forms the basement for the Kiraz

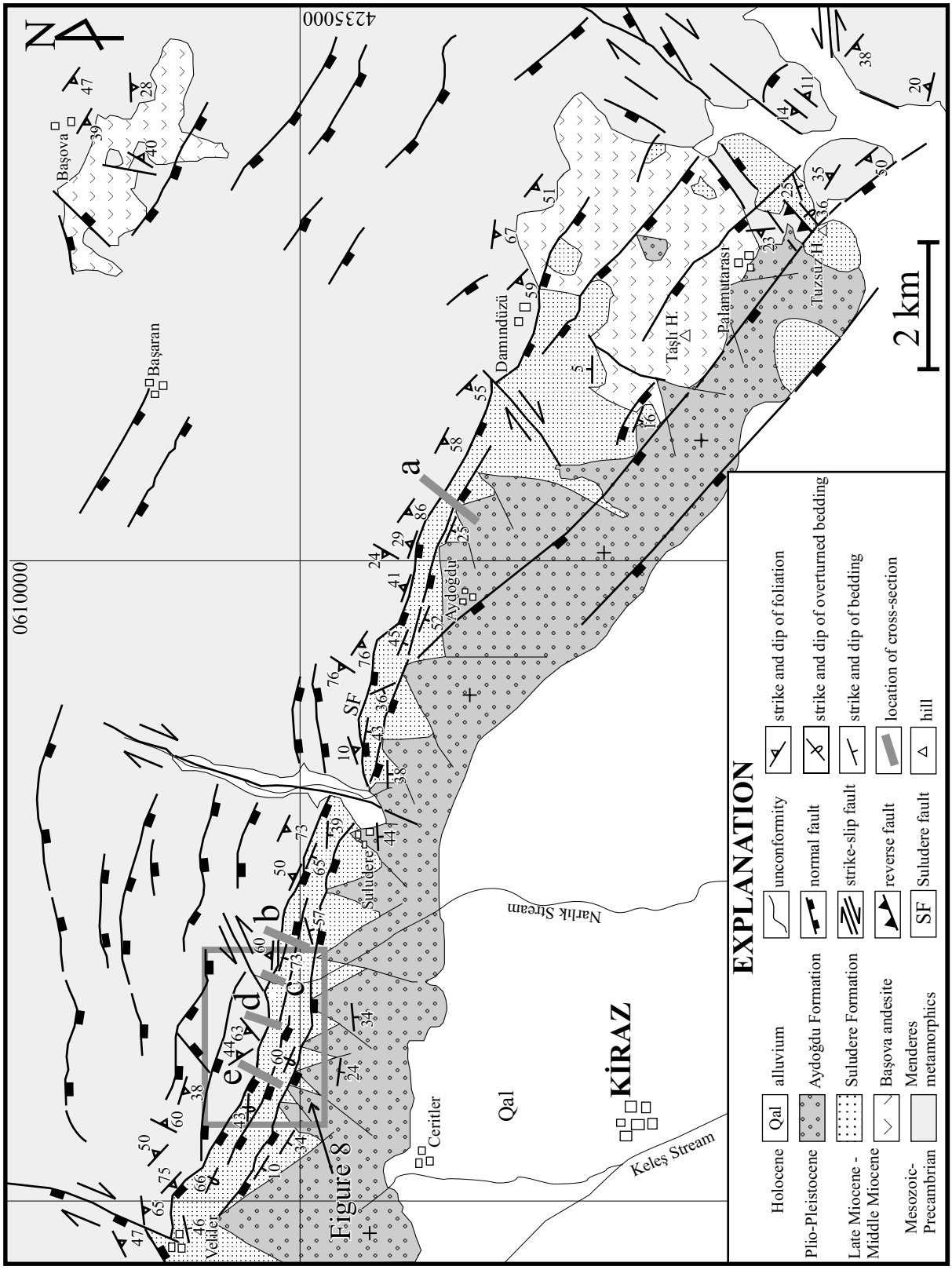

Figure 4. Detailed geological map of the Kiraz region (see Figure 3 for location and explanation).

Basin (Emre & Sözbilir 2005). Readers are referred to a recent study by Bozkurt & Rojay (2005) for a detailed description of the metamorphic basement rocks which crop out in the study area.

Young volcanic rocks (*Başova andesites)*, which cut the metamorphic rocks, exposed in three separate places (e.g., Başova, Karaburç and Yenişehir locality) but derived from the same magmatism, are Middle Miocene in age (Emre & Sözbilir 2005). Sphereoidal weathering is characteristic in these volcanic rocks. They occur as dikes, lavas, pyroclastic and volcanic breccias. The pink and grey andesitic rocks of the Başova and Karaburç areas have hyprocrystalline porphyritic texture, but are locally hyalopilitic. These rocks are made up of andesine, hornblende, pyroxene, biotite, quartz and opaques as essential minerals within a matrix of glass and plagioclase microlites. In the dark grey to greenish-grey, fine-grained basaltic andesites of the Yenişehir area, plagioclase and pyroxene phenocrysts in microlitic groundmass can be identified at outcrop scale. The microlites show no obvious orientation, but locally microlites encircle some phenocrysts. On the basis of $^{40}Ar/^{39}Ar$ radiometric age determinations, samples taken from Aykıran Tepe yielded an age of 14.7±0.1 Ma, and those from Yenişehir, an age of 14.3±0.1 Ma. More details about petrographic and geochemical features of the Başova andesites are given in Emre & Sözbilir (2005).

Basin-fill Units

Basin-fill units that unconformably overlie the metamorphic and volcanic rocks comprise the Upper Middle Miocene–Upper Miocene Suludere Formation, the Plio–Pleistocene Aydoğdu Formation and Holocene alluvium (Figures 3, 4 & 5).

Suludere Formation

The Suludere Formation unconformably overlies the metamorphic rocks of the Menderes Massif and the Başova andesites, begins with basal conglomerates that locally have a poorly sorted clayey-sandy matrix, but elsewhere are carbonate-cemented (Figure 6). Bedding in the conglomerates is unclear and sorting is poor. In the basal conglomerate, the clasts are basement-derived and angular in shape, with dimensions ranging from 2–3 mm to 50 cm. 600 m north of Taşlı Tepe, overlying the andesites, the poorly sorted and bedded carbonate-cemented conglomerate contains angular clasts which are predominantly of andesitic composition. The Suludere Formation is unconformably overlain by the Aydoğdu Formation and alluvium.

700 m NNW of Taşlı Tepe, a sandstone-dominated sequence commences with a basal conglomerate followed upward by a limestone-mudstone alternation (Emre *et al.* 2006). Pebbly sandstone, conglomerate and mudstone lenses and interbeds are common within the sandstones; their thicknesses do not exceed 15 cm, while lateral extent of mudstone and claystone lenses is about 1–2 m. The thicknesses of clayey to sandy limestone lenses and interbeds are less than 25 cm. In algal limestone-clayey limestone-cemented horizons, grain size varies between 4–5 mm and 50–60 cm; grains are coated and cemented by algal limestone. In sections where pebbles/cobbles are rare, white to beige limestones comprise stacked algal bioherms. Cobbles, of mostly marble, with sizes less than 15 cm, lie within a medium- to coarse-grained sandy matrix.

1.5 km NE of Beydağ (north of Aktepe Village), the sequence is composed of moderately indurated mudstones and sandstones. It begins with mudstones at its base, and continues upward with intercalations of conglomerate, conglomerate-sandstone and sandstone-mudstone. Locally, the conglomerate grades into sandstone, and sandstone into mudstone. Pebbles are poorly rounded to subangular with sizes <1 cm, and are characterized by low sphericity.

In exposures 250 m north of Suludere Village, the unit comprises mainly sandstone, mudstone and conglomerate. It begins with sandstone and mudstone, and continues upward with conglomerate, pebbly sandstone and sandstone; is capped by conglomerate. Lens-shaped conglomerates occur as 15–28-cm-thick bodies. Grain size varies between 2–3 mm and 50 cm, with a dominant size of 2–6 cm in the conglomerates and pebbly sandstones.

Age. Fresh-water ostracoda identified in these sediments (Emre *et al.* 2006) suggest a latest Middle Miocene–Late Miocene age. The palaeontological age assignment is in agreement with the available radiometric age data from the unconformably underlying Başova andesites (14.7±1 to 14.3±1 Ma Ar-Ar age, Emre & Sözbilir 2005).

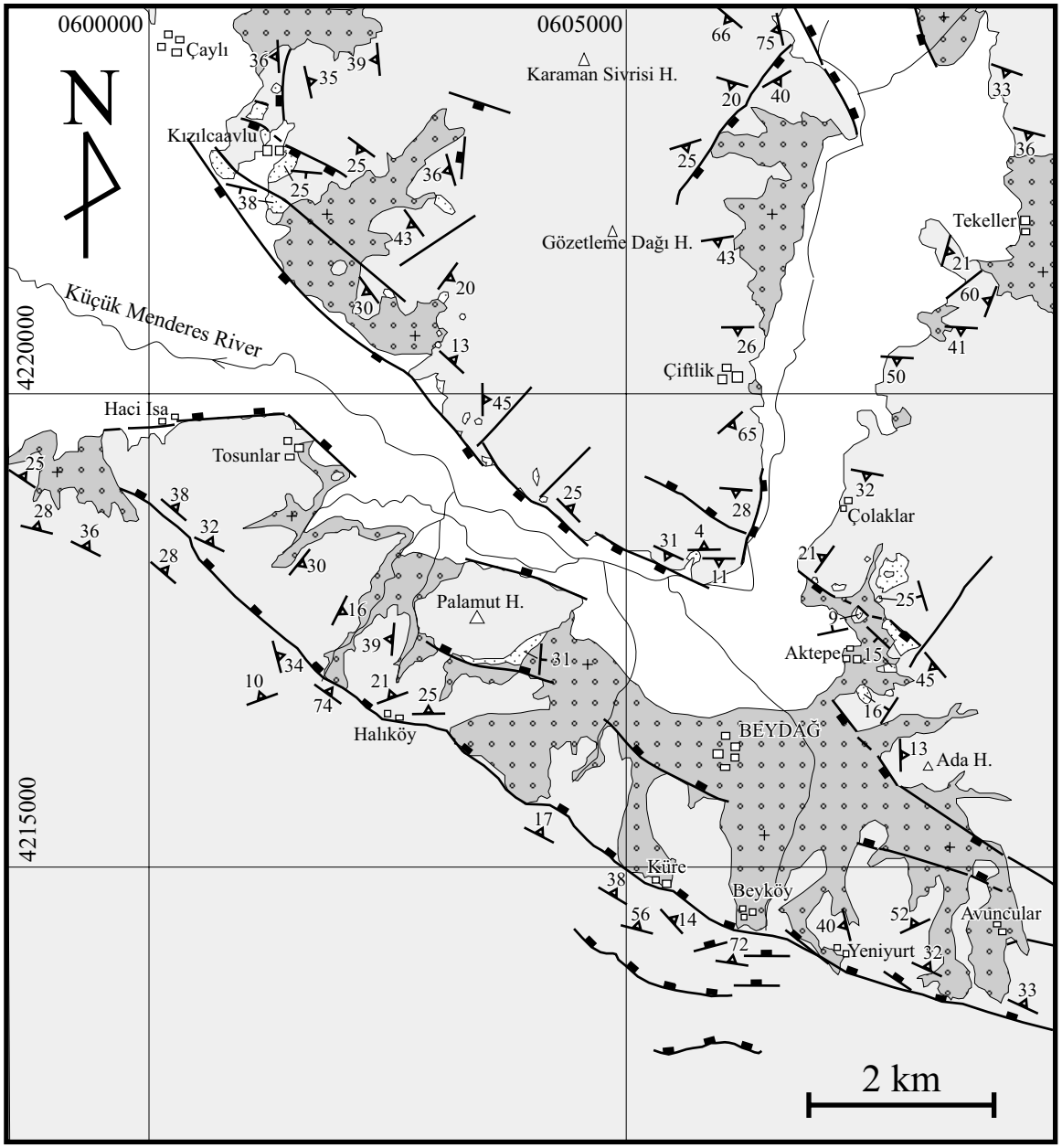

Figure 5. Detailed geological map of the Beydağ region (see figure 3 for location and explanation).

Description of Lithofacies. The conglomerates are yellowish, cream, beige and grey coloured, weakly to moderately (locally strongly) indurated, and moderately, thickly to very thickly bedded. Although generally moderately mature, locally these sediments are texturally immature or mature, and have sorting that ranges from very poor to good. Locally, these rocks are characterized by coarsening upward or normal grading. The conglomerates pass upward into pebbly sandstones, and finally into sandstones. Sphericity of the clasts is low, and they are mainly angular, subangular or slightly rounded, but in places are extremely angular or rounded and, locally, platy. The amount of clasts ranges from 20 to 80%, and their dimensions range from a few mm to blocks (up to a dimension of 80–90 x 60 cm). Almost all clasts are derived from metamorphic rocks. Andesite

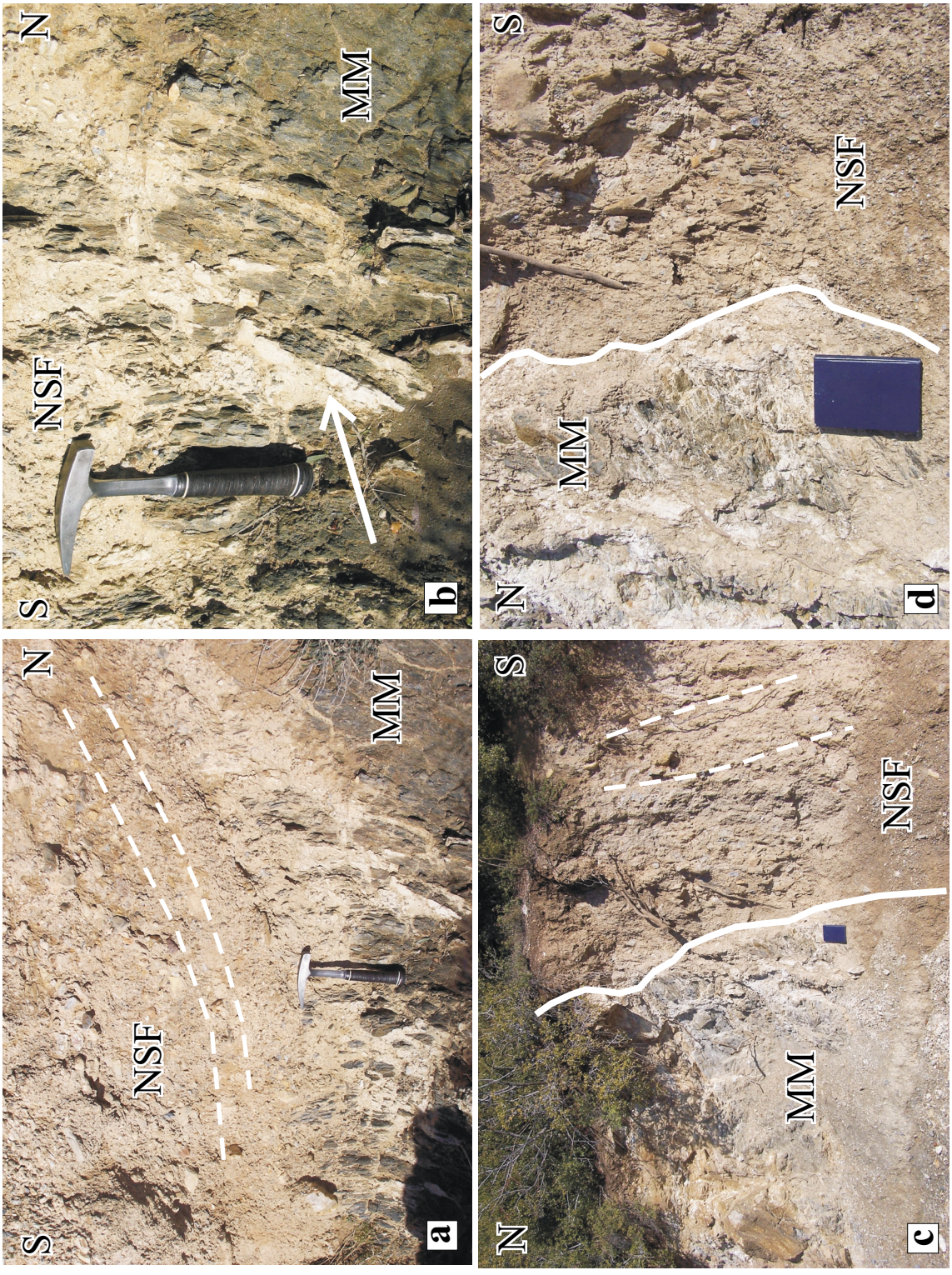

Figure 6. Field photographs of the main unconformity between metamorphic rocks of the Menderes Massif (MM) and the overlying Miocene sediments of the Suludere Formation (NSF). (**a**) Note appearance of gradual transition from metamorphic rocks to Miocene sediments suggests sedimentation without erosion at the beginning of the basin formation. Close up view of the carbonate infiltration (white arrow) into the cracks and schistosity planes of the schist unit. The same unconformity became steeply dipping towards the west (**c**) and here similar carbonate infiltration exists too (**d**). The hammer in (a) and (b), 32 cm long and the notebook in (c) and (d), 20 cm long.

clasts occur locally, but they never make up more than 1% of the rock. The predominant type of metamorphic clasts varies in relation to the source area. In places, 60% are marbles, 20–30% are schists with lesser quartzites, or 60% schists and 20–30% marbles; elsewhere, the clasts are 60–90% gneisses with the remainder schists and quartzites, or locally 45% schists and 50% gneisses. The matrix- or grain-supported conglomerates, are generally characterized by fine to coarse sand-, fine pebbles-coarse sand-, or locally clayey-sandy matrix; at the base of the sequence the conglomerates are algal limestone or clayey-silty-sandy-carbonate-cemented. The sandstone and pebbly sandstone interbeds and lenses of varying thickness occur locally. In some sections, conglomerate levels with differing degrees of induration or sorting follow each other, or elsewhere, lenses of poorly sorted conglomerates are present within well-sorted conglomerate. The long axes of rounded clasts or the broad surfaces of platy clasts are parallel to the bedding.

The sandstones are of variable colour (grey, cream, beige, greenish or milky brown), weakly to moderately (locally strongly) indurated, generally fine- but locally very fine- or medium/coarse-grained, and medium–thick bedded (but in a few places laminated thin- or very thick-bedded). In general, they display regular bedding, and show local upward fining sequence. In places, at the base of this unit, pebbly coarse-grained sandstones grade upward into fine-grained sandstone, or elsewhere into claystone or clayey-sandy limestone. Sandstones locally contain bird's-eye voids; the presence of angular andesite clasts, oval carbonate nodules, and abundant mica flakes give the sandstone a black-grey-spotted appearance. The sandstones are locally intercalated with conglomerates or mudstones. In places, they also contain interbeds or lenses of pebbly sandstone and conglomerate, and elsewhere scarce claystone, cream-coloured clayey limestone or limestone.

The pebbly sandstones are light greenish-grey, light brick red or light brown coloured, moderately to strongly indurated, moderately to well-sorted, and medium–thick bedded. They are gradational into, or are intercalated with, sandstones and conglomerates; they also contain local mudstone interbeds. The dimensions of scattered pebbles/cobbles within the medium- to coarse-grained sandstones vary between 3 mm and 5–10 cm, with a dominant size of 2–3 cm up to 5–6 cm. These rocks contain scarce andesite (<5 cm) clasts or 8–10-cm-long platy schist clasts. The long axes or broad surfaces of platy clasts are parallel to the bedding.

The claystones and mudstones are grey, beige, reddish, light brown, light grey or greenish grey, generally weakly-moderately (locally strongly) indurated, medium–thick bedded, and locally thinly bedded or laminated and show low durability. The mudstones and claystones are locally intercalated and/or occur as lenses or interbeds within the each other. The mudstones, locally intercalated with clayey limestone or sandstone, contain sandstone, conglomerate, pebbly sandstone, pebbly mudstone, clayey limestone or limestone lenses or interbeds. Within the claystones and mudstones, scarce *Planorbis* sp. fossils, calcareous nodules or scattered pebbles occur.

The limestones are beige, cream, light grey and milky brown, thin–medium and thick bedded; they form resistant lithologies. They contain algae-enclosed reed stems, intraformational pebbles, oval limestone nodules, spherical algal bioherms (measuring from 3–5 cm to 25 cm in diameter), oncoidal stromatolites, and fossils of pelecypod and *Planorbis* sp. Some of the voids that developed via the decay of the algae-encrusted reed fossils or other plant fragments are filled with calcite crystals. In some sections, limestones are spotted, silicified and contain dendritic manganese-oxide. Algal limestones are made up of stacked algal bioherms or hemispherical stromatolites, and are laterally gradational into sandy or clayey limestones.

Laterally transitional into algal limestones, sandstones and mudstones, sandy and clayey limestones are locally intercalated with mudstones. Light grey-beige clayey limestones, with beds 2–30-cm thick, locally contain 1–2 mm bird's eye voids, plant stems, or 2 mm to 3–4 cm angular to subangular schist and andesite clasts.

Intrepretation of Lithofacies. In many places atop the basement, following an initial limestone-clayey limestone-cemented basal conglomerate, the formation continues upward with limestone-clayey limestone and mudstone levels containing planktic and benthic foraminifera and fresh-water fossils (Emre *et al.* 2006). The fossil content shows that the deposition of Suludere Formation began in a low energy, shallow-lake environment that was influenced by the open sea. Lithological variation was

related to the amount of clay and silt influx that reached the lakes. The aforementioned ?foraminifers are extremely poorly preserved, and must have been transported into the depositional environment of the Suludere Formation by surface streams in communication with the open sea. In upper levels, the presence of increasingly more fresh-water ostracods suggests that, in later periods, the contribution of the open sea to the coastal lakes ceased.

The sediments lying atop the limestones comprise successive fillings of low-energy river channels and flood plains, and were deposited in a slightly sloping topography. In this period, the slope of the topography was slight enough to allow development of flood plains, and the energy of the flowing water in this slightly sloping topography was low enough to be appropriate for the settling out of material suspended in the water. Mudstones, overlying the sandstones and conglomerates, were deposited above channel fills as a result of the lateral migration of river beds or river-bed replacement (Emre *et al*. 2006). Among the clastics, the limestone and clayey limestone levels show that flood plains remained stable over a period sufficient for limestone precipitation and that, during this process, the introduction of clastic material decreased significantly.

The decrease in mudstones and claystones, and the increase in conglomerates and pebbly sandstones, suggest increases in the slope of the topography and in stream energy. These sediments were deposited under the control of steep topography and high-energy waters. The variably well- and poorly-sorted conglomerate levels indicate sudden changes in stream energy. On the basis of the textural and geometric characteristics of the conglomerates, we can say that these rocks developed in a stream-controlled alluvial-fan environment rather than as debris flows.

The sandstones that overlie the conglomerates show that the current energy decreased over time. Mudstone or coarse conglomerate lenses within the sandstones can be explained by the development of bar-top sedimentation and/or local energy changes in the stream channel. Reverse/normal grading locally observed in the sandstones and conglomerates indicate progressive increase/decrease in water energy. The absence of spores and pollen in this unit is in agreement with the proposed depositional environment.

Aydoğdu Formation

The Aydoğdu Formation is underlain by Menderes Massif metamorphic rocks, the intrusive Başova andesites and the Suludere Formation, and is overlain by Quaternary alluvium with an angular unconformity. Conglomerate at the base of the formation are very poorly sorted, lack obvious bedding and have a matrix made up of coarse sand and small pebbles. The clasts are angular and range in size from a few cm up to boulders (2–3 m).

This formation is exposed over a total of 35 km^2 in the Beydağı, Uzundere, Çaylı, Aydoğdu, Gedik and Ceritler areas, with the best outcrops occurring in the Aydoğdu (northeast of Kiraz) area (Figure 3, 4 & 5). This formation is generally reddish brown, milky brown, or locally yellowish grey and comprise texturally immature conglomerates, pebbly sandstone and sandstone. These lithologies are mutually transitional, both laterally and vertically, and their contacts are locally graded, elsewhere sharp. Conglomerates predominate over sandstones. As a result of rapid erosion, this weakly indurated formation is locally characterized by steep slope and fairy-chimney morphologies. The Aydoğdu Formation is mainly horizontally bedded.

The sequence northwest of Eselli comprises mainly sandstones and conglomerates. These sediments, which begin with conglomerates, contain medium–thick-bedded sandstone levels and are capped by thick to very thick-bedded pebbly sandstones. Grain size in the conglomerates is generally in the range of 5–20 cm.

The section measured at Çaylı comprises mainly conglomerates and sandstones. At its base, scarce coarse-grained pebbly sandstone occurs, and the sequence continues upward with intercalated conglomerate and sandstone.

Age. The Aydoğdu Formation, which has yielded no palaeontological data whatsoever, is accepted as Plio–Pleistocene in age insofar as it unconformably overlies the upper Middle Miocene–Upper Miocene Suludere Formation.

Description of Lithofacies. The conglomerates, whose colours vary between light brown and dark reddish brown, are moderately to strongly indurated and medium–thick to very thick bedded. Bedding thickness

varies between 20 cm and 500 cm, but is mainly in the range of 25–50 cm, 100–170 cm and 300–500 cm. In these generally immature-partially mature and very poorly- to poorly-sorted rocks (but that are locally mature and moderately to well-sorted), clasts are mainly angular to subangular – locally sharply angular or platy – where sphericity is low. Clasts, though mainly of metamorphic derivation, also include scarce andesite clasts (maximum 30 x 20 cm). In terms of frequency, the clasts are schist (70%), gneiss (25%), and marble (5%), but locally are 80–95% gneiss or 90% schist. Clast sizes range from 3–4 mm up to 60 cm, but scarce boulders (1–3 m) are also encountered. In general, grain size coarsens upward, and the conglomerates are characterized by a chaotic internal structure. Locally, clasts are arranged in a building-block fashion. Coarse-grained sandstone lenses of moderate thickness occur locally. Scarce cross-bedding, channel fills, scour-and-fills and syn-depositional faults have also been observed.

Sandstones are generally light brown or locally reddish brown, moderately indurated, generally coarse-grained and medium–thick bedded, with regular bedding. Bed thicknesses vary between 20 cm and 200 cm, but are mainly 30–60 cm and 80–100 cm. At the base, the scattered-pebble coarse-grained sandstones are characterized by fining upward bedding.

Pebbly sandstones are light brown to reddish brown, moderately indurated, and thick- to very thick-bedded. Within the sandstones, scattered pebbles make up <5% of the rock. In some levels, grain size does not exceed 3–5 cm, but elsewhere is 30–40 cm.

Interpretation of Lithofacies. Deposition of the Aydoğdu Formation in front of the Suludere fault zone to the north and the Halıköy Fault to the south produced alluvial fans with axes oriented approximately N–S and NE–SW (Figure 4 & 5). The presence of sand-sized clastics together with huge blocks within the conglomerates, are indicative of deposition in a environment from a high-energy flow capable of sudden load dumping, with generally large clasts oriented according to flow direction with smaller pebbles and sand-sized material deposited in the lower parts. In some sections, the presence of grading indicates decrease in flow velocity over time.

Scattered pebbles within the sandstones, variable thickness of bedding, and the lack of sedimentary structures tied mainly to current direction, show that these rocks formed from hyperconcentration or debris flows. Scarce current-related sedimentary structures formed in periods when flow velocity was, relatively speaking, slightly decreased and the flow regime regular.

Alluvium

The youngest depressions in the study area continue to be filled by alluvium, and these topographically low areas comprise broad plains. These grey-beige, unindurated clastic sediments, comprising material of varying grain size collected by present-day streams, unconformably overlie all other units.

Structural Geology

We have grouped the structural elements under two main headings: (a) contractional and extensional structures developed within the metamorphic basement that pre-date the basin formation, and (b) structures that play key role during the basin formation. Structural data from these have been evaluated in Angelier's program (Angelier 1984, 1991, 1994, see Table 1).

Structures Pre-date the Basin Formation

Two types of structures are observed within the metamorphic basement rocks of the Kiraz Basin. The older one is recorded at the footwall rocks of the Beydağ Fault, to the northwest of Beydağ Village. There Mesozoic marble is thrust over the schist unit. Kinematic indicators developed in the underlying schist unit suggest top-to-the-north sense of shear (Figure 7a–c). This top-north deformation may have resulted in imbrication of the Menderes Massif (Bozkurt & Rojay 2005). Northward tectonic transport by thrust faulting throughout the Menderes sequence has also been documented by Hetzel *et al.* (1998) and Lips *et al.* (2001). The timing of this tectonic event has been interpreted to be Pan-African (Ring *et al.* 1999) or Alpine (Hetzel *et al.* 1998; Lips *et al.* 2001; Bozkurt & Rojay 2005) in age. The younger deformation is established in the footwall rocks of the Halıköy Fault, to the South of Beyköy Village, where gently to moderately south-dipping extensional shear band foliation is observed (Figure 7d). The fabric suggests a top-to-the-southwest movement that is consistent with the footwall structures of the Büyük

Table 1. Measurements of slickensides and slickenlines, which belong to the studied faults in the Kiraz Basin.

strike (°N)	dip angle & direction (°)	rake (°)	nature of fault	principal stress axes	Φ
sinistral strike-slip fault					
055	85S	30W	sinistral		
050	82S	32W	sinistral		
052	85S	25W	sinistral	$\sigma_1 = 186^o/09^o$	
050	86S	30W	sinistral	$\sigma_2 = 087^o/42^o$	0.268
048	80S	30W	sinistral	$\sigma_3 = 285^o/47^o$	
050	84S	28W	sinistral		
051	83S	27W	sinistral		
reverse fault					
110	65N	58W	reverse		
130	65N	35W	reverse		
130	38N	50E	reverse	$\sigma_1 = 331^o/16^o$	
145	40N	45E	reverse	$\sigma_2 = 087^o/04^o$	0.356
100	58N	65W	reverse	$\sigma_3 = 135^o/73^o$	
105	75N	60W	reverse		
dextral strike-slip fault					
022	63E	03S	dextral		
026	66E	05S	dextral		
025	65E	02S	dextral	$\sigma_1 = 259^o/18^o$	
034	63E	05S	dextral	$\sigma_2 = 110^o/69^o$	0.700
030	59E	02S	dextral	$\sigma_3 = 352^o/10^o$	
028	68E	02S	dextral		
Suludere Fault					
115	62S	65W	normal		
120	64S	72W	normal		
115	66S	65W	normal		
113	66S	68W	normal	$\sigma_1 = 314^o/70^o$	
090	70S	60W	normal	$\sigma_2 = 120^o/19^o$	0.195
095	72S	73W	normal	$\sigma_3 = 212^o/04^o$	
115	62S	88W	normal		
120	60S	70W	normal		
110	63S	60W	normal		
Halıköy Fault - Beydağ Fault					
120	50S	70W	normal		
103	33S	83W	normal		
100	45S	89W	normal		
115	38S	89W	normal		
118	58S	78W	normal	$\sigma_1 = 342^o/86^o$	
110	55S	80W	normal	$\sigma_2 = 110^o/02^o$	0.531
090	70N	70E	normal	$\sigma_3 = 200^o/03^o$	
120	57N	75W	normal		
105	55N	73E	normal		
120	72S	60E	normal		
112	74S	58E	normal		
115	42S	86E	normal		

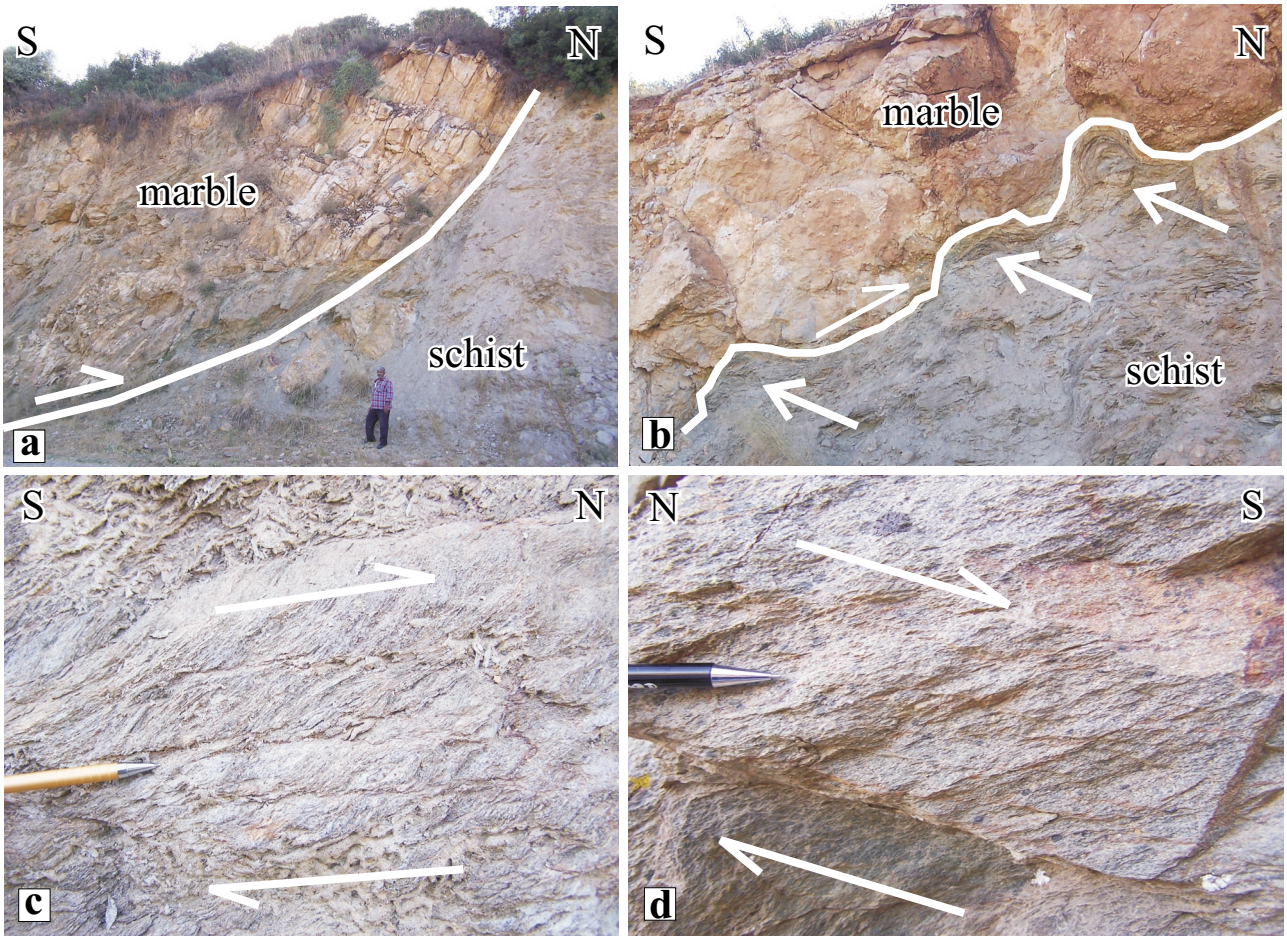

Figure 7. Field photographs of the contraction- (a, b, c) and extension-related (d) structures that developed within the metamorphic basement and that pre-date formation of the Kiraz Basin. (a) Thrust fault between highly brecciated marble unit and the underlying schist unit. Note meso-scale folds developed just under the thrust planes (b); and shear-band foliation within the underlying schist unit showing top-to-the-north sense of shear (c). (d) Close-up view of the extension-related shear band foliation that developed within the uppermost part of the footwall of the Halıköy Fault. Note the brittle deformation confined to narrow zones and top-to-the-south sense of shear. The man in (a), 180 cm tall.

Menderes detachment fault forming during the regional extensional collapse of the central Menderes Massif as previously recorded by Lips *et al.* (2001). Detailed description and interpretation of these structures are given in Hetzel *et al.* (1998) and Bozkurt & Rojay (2005).

Structures Shaping the Kiraz Basin

Structures shaping the Kiraz Basin fall into four main categories: (1) reverse fault, (2) strike-slip fault, (3) high-angle normal fault and (4) intraformational unconformities. Three main systems of faults are present throughout the basin. The first one is a set of NW–SE-striking normal faults which occur primarily at the northern and southern boundaries of the Kiraz Basin. The second is a system of NE-trending strike-slip faults which are pervasive at the western, middle and eastern end of the northern margin of the basin. Within a local area, between Suludere and Veliler villages, contractional deformation recorded by reverse faults was also established.

Reverse Fault

This fault occurs at the northern margin of the Kiraz Basin between Suludere and Veliler villages (see Figure 8 for detail). It is approximately 1.5 km in length and

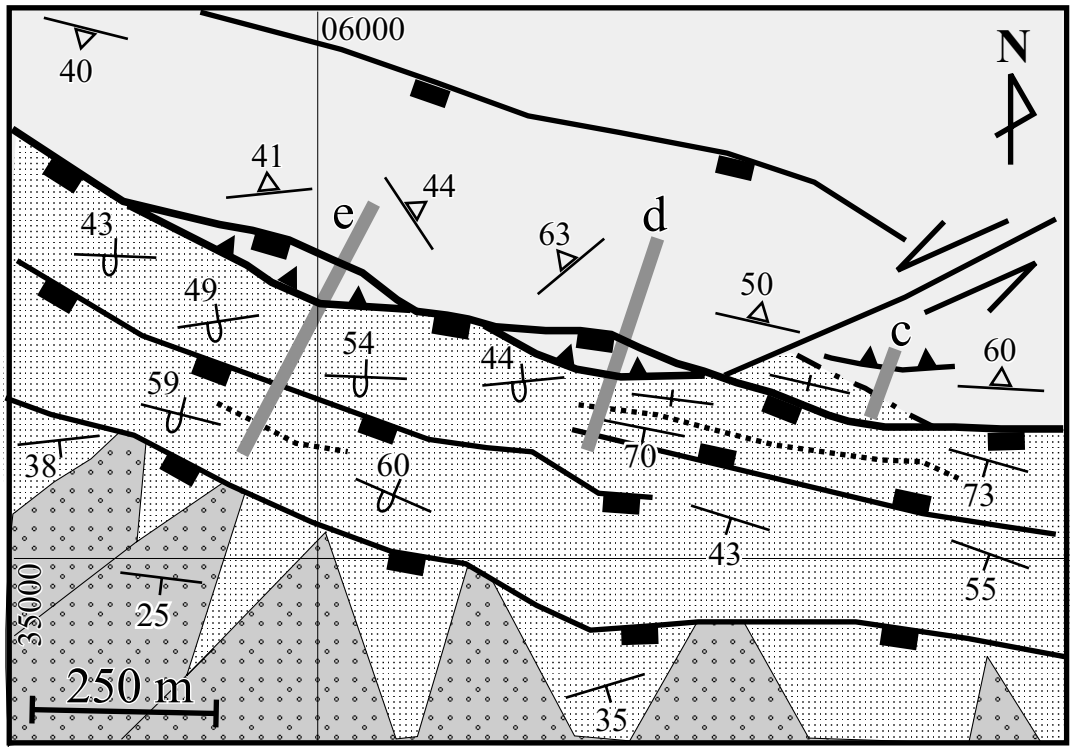

Figure 8. Detailed geological map of the area showing contact relationships between the Suludere Formation and metamorphic rocks of the Menderes Massif. Note presence of overturned bedding and intraformational unconformities close to the contact. See Figure 4 for location and explanation.

displays a curvilinear fault trace. Across the fault, marble-schist units of the Menderes Massif are thrust from northwest to southeast over the overturned clastic beds of the Suludere Formation (Figure 9). Close to this contact, several compression-related reverse faults and folds can also be observed within the metamorphic basement (Figure 9b–d). The reverse fault, however, is masked, displayed and overprinted by a high-angle normal fault (Suludere Fault) and thus it is therefore difficult to be mapped at the scale of 1/25 000. Generally Miocene strata are steeply to moderately overturned to the north, consistent with the geometry of the reverse fault. Indeed, the along-strike gradual transition from overturned to vertical and to low-angle dipping of strata matches the eastward decrease in displacement along the fault. There is no evidence for the presence of a thrust or reverse fault between the Menderes Massif and Suludere Formation at the eastern continuation of the Suludere Fault except at the Tuzsuz Hill locality. At this locality (see Figure 4), metamorphic rocks of the Menderes Massif (marble unit and slices of the schist unit) is in reverse fault contact with the carbonate-clastic rocks of the Suludere Formation (Figure 9e & f). This NE-trending reverse fault can only be traced within a very small area bounded from the northern and southern sides by NW-trending high-angle normal faults.

The reverse motions on these fault is consistent with approximately N–S compression; the calculated σ_1 trends in 331° and plunges gently at 16°, whereas σ_2 and σ_3 axes have attitudes of 087°/04° and 135°/73°, respectively (Table 1, Figure 10).

Strike-slip Faults

Strike-slip faults occur especially at the eastern and western termination of the Suludere Fault. The NE-trending fault zone located between Karaburç and Tuzsuz Hill, along the Pınar Dere, is 200 m wide and comprises a 2-km-long dextral strike-slip fault zone. Here, several nearly horizontal slickenside striae on fault planes cutting the metamorphic foliation are observed. There are few locations where the intersection relationships between

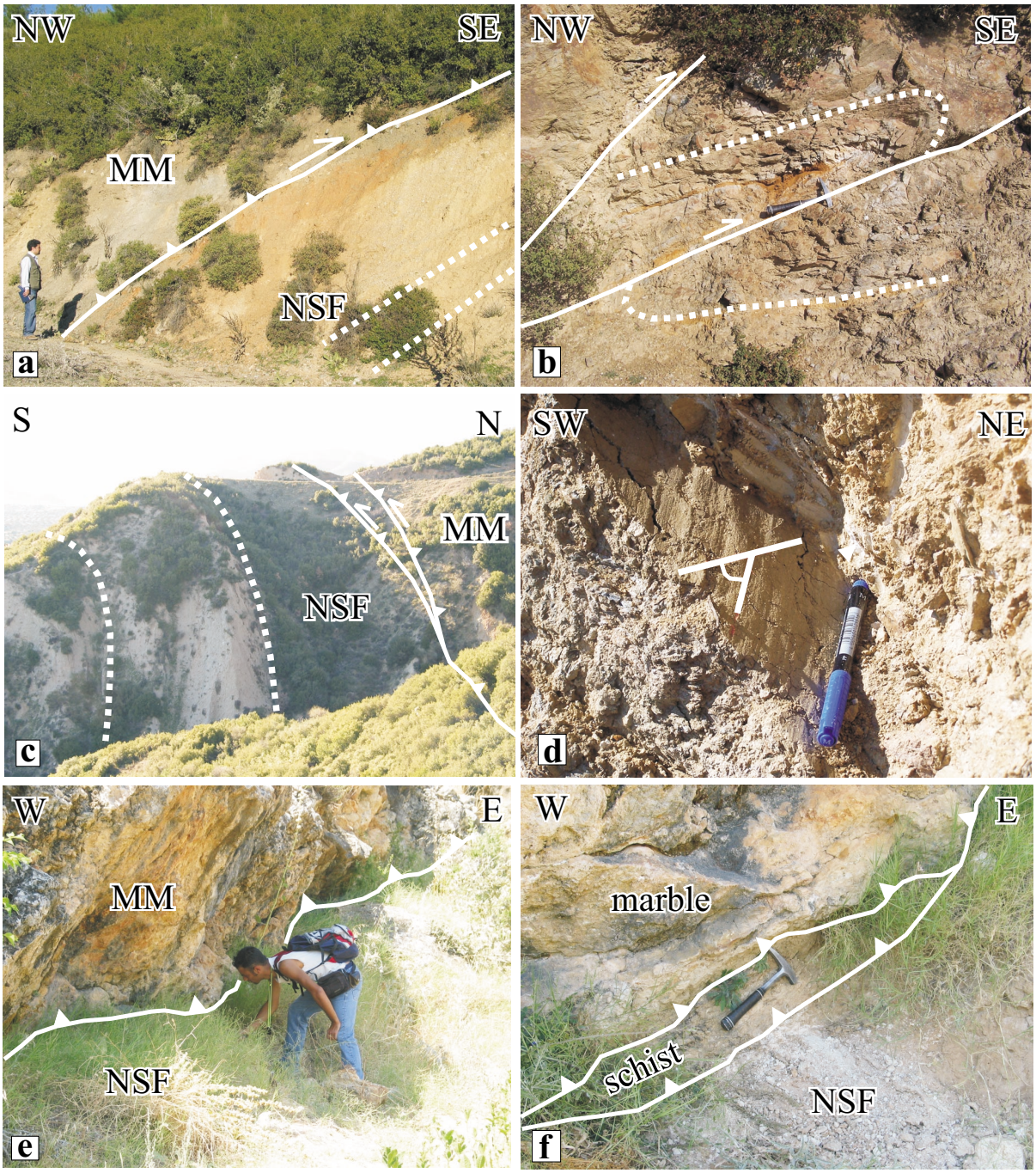

Figure 9. Field photograps showing meso-scale compressional structures associated with reverse faults that post-date sedimentation of the Suludere Formation. **(a)** Metamorphic rocks of the Menderes Massif in reverse fault contact with the overturned Miocene basin sediments. Turkish UTM coordinate: 06075°E / 35290°N. **(b)** Schistosity showing an overturned fold is cut and displaced by a brittle reverse fault. This photograph is taken from western end of the former photograph very close to the contact-forming reverse fault. **(c)** High-angle to reverse structural contact between metamorphic rocks of the Menderes Massif and the Suludere Formation. Note upward overturning bedding of the Suludere Formation due to southern motion of the hanging-wall block. Turkish UTM coordinate: 06245°E / 35210°N. **(d)** Detail of slip surface within the breccia zone showing oblique-slip slickensides. Asymmetric structures located within the brecciated zone indicate reverse motion on this fault. Turkish UTM coordinate: 06880°E / 35150°N. **(e)** Marble unit belonging to Menderes Massif is in reverse fault contact with Miocene sediments of the Suludere Formation. Note small slices of schist unit between the marble unit and the Miocene sediments **(f)**. Turkish UTM coordinate: 12677°E / 31157°N. The man in (a), 170 cm tall, the hammer in (b), 32 cm long, the pencil in (d) and (f), 12 cm long, and the man in (e), 182 cm tall.

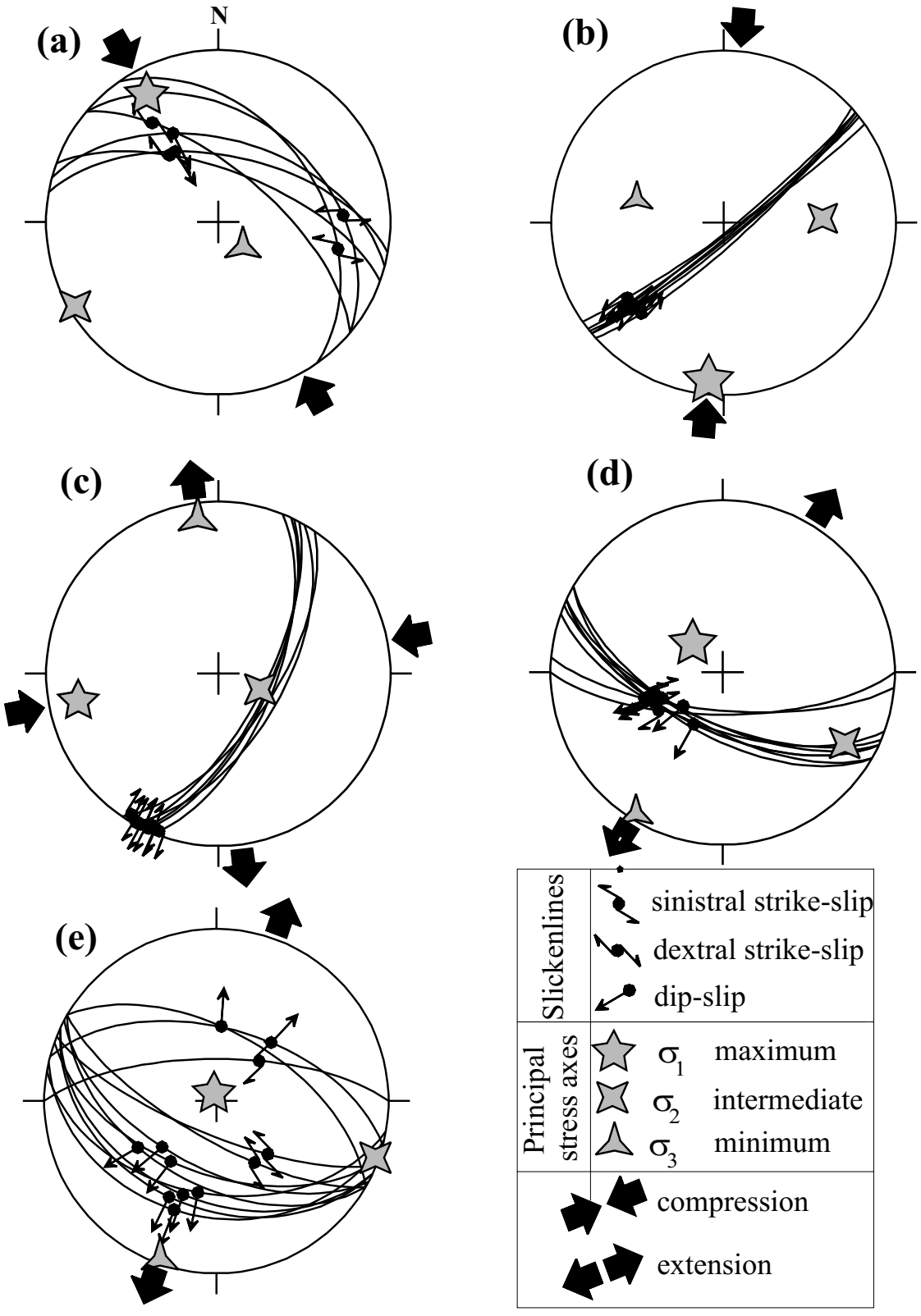

Figure 10. Lower hemisphere equal area projection of the studied faults. Great circles show fault planes and the arrows are striations.

the NW-trending normal faults and NE-trending strike-slip fault can be observed. Where the two fault sets intersect, the NW-trending faults either terminate against or cut into the NE-trending faults. These key relationships indicate that the NE-trending strike-slip fault accommodate N–S strain during the basin formation and are later cut by younger NW-trending normal faults.

Palaeostress data obtained from the NE-trending dextral strike-slip fault zones indicate approximately N–S extension associated with E–W compression. The estimated intermediate principal stress axis (σ_2) plunges steeply at 69° and trends in 110°. The calculated maximum and minimum principal stress axes, σ_1 and σ_3 are 259°/18° and 352°/10°, respectively (Table 1, Figure 10).

There are also several basement-involved sinistral strike-slip faults located especially between Suludere and Veliler Village (see Figure 4). These brittle faults have highly brecciated and wide fault zone with well-defined fault surfaces showing en-échelon pattern (Figure 11). Slickensides on these slip planes indicate oblique to pure strike-slip motion. The sinistral slip along the basement-involved strike-slip faults may be interpreted as a result of N–S shortening as obtained from the palaeostress data (Tabel 1, Figure 10). The average orientations of the principal stresses and stress ratio for the strike-slip faults are; σ_1= 186°/09°, σ_2= 087°/42°, σ_3= 285°/47° and Φ= 0.268, indicating N–S compression in accordance with the palaeostress data obtained from the reverse fault. This result suggests that the strike-slip faults may have accommodated compressional strain during the reverse faulting.

High-angle Normal Faults

Numerous high-angle normal faults of varying sizes are mapped at both the northern and southern margins of the basin. These faults are dip to oblique slip in nature, and they range in length from 50 m to 10 km. They juxtapose the metamorphic rocks of the Menderes Massif with Neogene to Quaternary sedimentary units. Step-like configuration of these faults can also be seen to the north of Kiraz and to the south of Beydağ (see Figures 4 & 5). The most important and longest of these faults are (1) NW–SE-oriented and north-facing Halıköy Fault and (2) NW–SE-oriented and south-facing Suludere Fault.

The Halıköy Fault is the southern basin-bounding fault that extended in a NW–SE direction and is located between Yeniyurt and Hacı İsa. It is a basin-facing normal fault, about 10 km long, and controlled alluvial sedimentation of the Aydoğdu Formation. Metamorphic schists comprising up-thrown southern footwall block, and mylonitic gneiss in the northern down-thrown block are tectonically juxtaposed along the fault (Figure 12a, b). The fault has a 1–20-m-thick clay gouge, and a few centimeter-wide cinnibar infilled veins (Akçay *et al.* 2006). Early workers interpreted the Halıköy Fault either as a thrust (Yıldız & Bailey 1987) or a normal fault (Akçay *et al.* 2006; Emre *et al.* 2006). The juxtaposion of two distinct metamorphic lithologies along the Halıköy Fault may suggest the fault is a reactivated structure with an early phase of thrust/reverse faulting and a later phase overprinting normal faulting with minor amount of dextral component (Figure 12c, d).

North of the Halıköy Fault, the NW-trending antithetic Beydağ Fault has relatively low-angle normal faults with respect to the other normal fault in the region. Computed results of fault slip data on the Halıköy and the Beydağ faults define an approximately vertical σ_1 trending in 342° and plunging steeply at 86° that is consistent with NE–SW extension. The average orientations of σ_2 and σ_3 are 110°/02° and 200°/03°, respectively (Table 1, Figure 10).

Suludere Fault

The Suludere Fault is the northern basin-bounding structure that can be followed from Veliler to Karaburç, north of Kiraz Town. To the west, the Suludere Fault appears to terminate near Veliler Village, while to the east, it is cut by a NE-trending strike-slip fault zone. The Suludere Fault is approximately 10 km long, NW-trending and south-facing range front fault. It consists of two closely parallel major fault segments, one of which marks the tectonic contact between the Menderes Massif and the Suludere Formation and cuts the Başova andesites, the other segment juxtapose the Suludere Formation with the Aydoğdu Formation. Numerous synthethic fault segments with variable length have been mapped in both the footwall and hanging wall of the Suludere Fault. The Suludere Fault displays triangular facets, poorly-preserved slickensides and step-like structural configurations at several localities (Figure 12e, f).

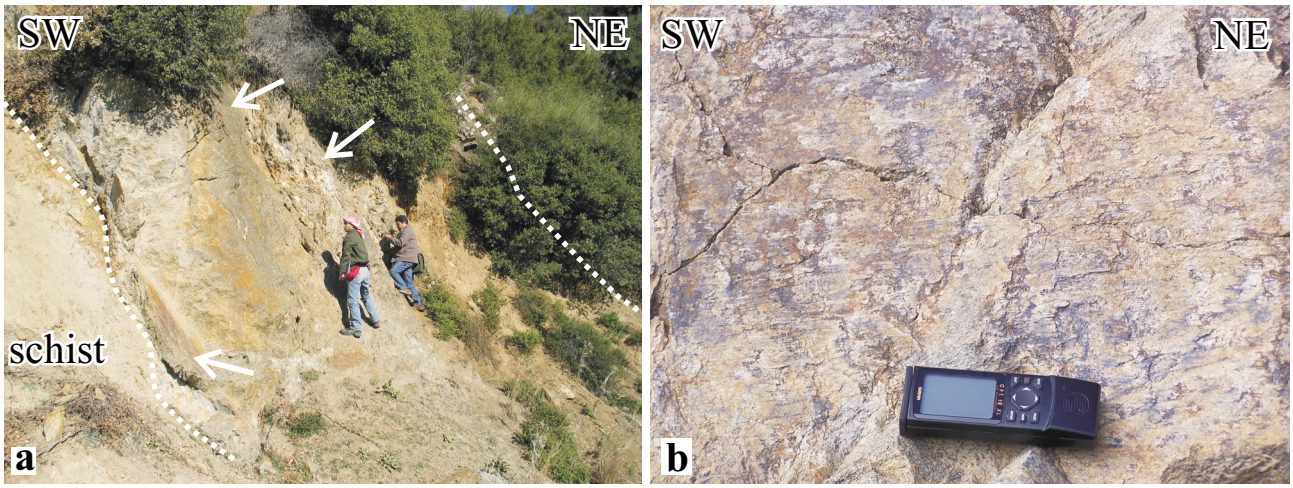

Figure 11. Field photographs of the NE-trending strike-slip faults. **(a)** The interior of the fault zone, composed of highly brecciated metamorphic rocks with well-defined fault-slip surfaces showing en-échelon pattern (white arrows). **(b)** Slickensides indicate nearly pure strike-slip motion on slip planes. Turkish UTM coordinate: 07972°E / 35240°N. The man in (a), 180 cm tall, and the GPS tool in (b), 14 cm long.

Kinematic analysis operated along the fault zone indicate that the Suludere Fault is a high-angle normal fault dipping at average 65°SW with a minor amount of sinistral strike-slip component. Computed results of fault-slip data define a steeply dipping σ_1 trending in 314° and plunging at 70° that is consistent with NE–SW extension (Table 1, Figure 10). The average orientations of σ_2 and σ_3 principal axes are 120°/19° and 212°/04°, respectively.

Intraformational Unconformities

In the studied area several syntectonic unconformities have been observed in the lower part of the Suludere Formation (see Figure 8). The most convincing evidence is given by the differences of the dipping degrees of the strata. The intraformational unconformity observed in the Suludere Formation are restricted to the marginal areas of the northern basin margin and they die out across the basin centre, where the sequence are thin, gently dipping and not affected by synsedimentary deformation.

Five representative field cross-sections have been studied from the northern margin of the Kiraz Basin in order to show the relationships between tectonics and sedimentation along the northern basin margin. At the easternmost section (Figure 13a), a low-angle unconformable contact (average dip is 31°) between the Miocene sediments and the underlying metamorphic rocks of the Menderes Massif is observed. Towards the nothwest, the steeply dipping (up to 80°) northern boundary of the basin and variation in dips of bedding within the Suludere Formation creates an intraformational unconformity (Figure 13b). Vertical to overturned basal unconformity associated with an oblique-slip reverse fault is established within the metamorphic basement, while towards the south gradual decrease in dips of bedding due to an intraformational unconformity (Figure 13c, d). Close to Veliler Village, an overturned intraformational unconformity is in good accordance with the reverse fault contact between the Menderes Massif and the underlying Miocene sediments (Figure 13e).

Syntectonic unconformities may have been related to three structural settings which progressively operated during the sedimentation of the Suludere Formation: (a) uplift associated with folding, (b) uplifting of push-up structures and/or (c) synsedimentary folding and thrusting. The progressive unconformity in the northern margin of the basin was defined using the model proposed by Riba (1976). According to this model, in the proximal areas of sedimentation rapid variation in the dip of the strata should be present. These internal unconformities may record the occurrence of rapid, and localised uplift contemporaneously with the sedimentation operating along the basin margin.

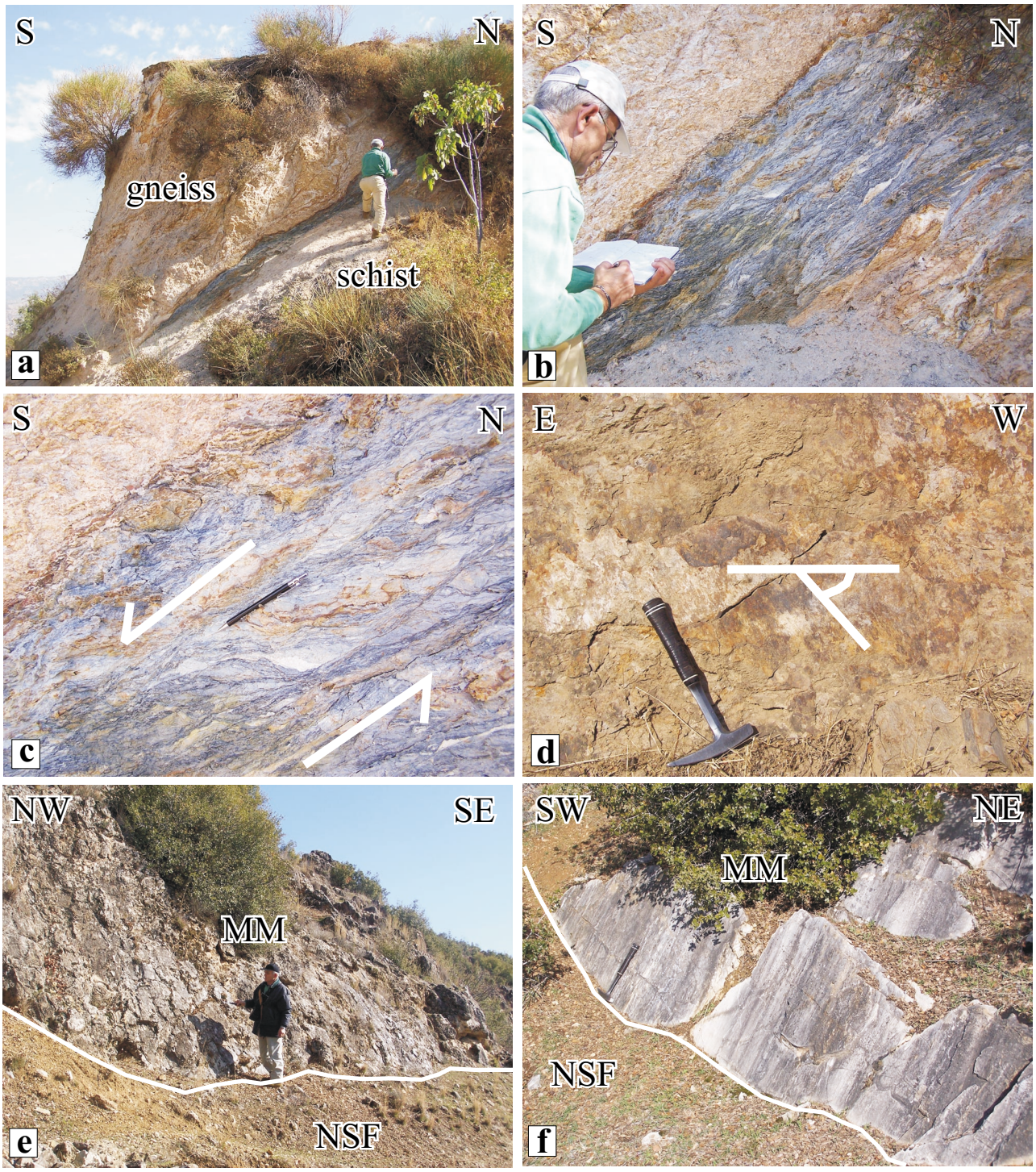

Figure 12. Field photographs of the high-angle normal fault faults. **(a)** An exposure approximately normal to the strike of the Halıköy Fault along which gneiss and the underlying schist unit are brought into contact. **(b)** The fault zone between gneiss and schist is characterized by well-developed asymmetric mesostructures showing top-to-the-northwest sense of shear **(c)**. **(e)** Close-up view of the fault zone. Note the rake of the slip lines suggests that motion along the Halıköy Fault is normal with minor amount of dextral component. **(e)** A fault scarp of the Suludere Fault along which the sediments of the Suludere Formation and marbles of the Menderes Massif are juxtaposed. **(f)** A close-up view of the Suludere Fault surfaces showing step-like structural configuration. The man in (a), (b) and (e), 170 cm tall, the pencil in (c), 13 cm long, and the hammer in (d) and (e), 32 cm long.

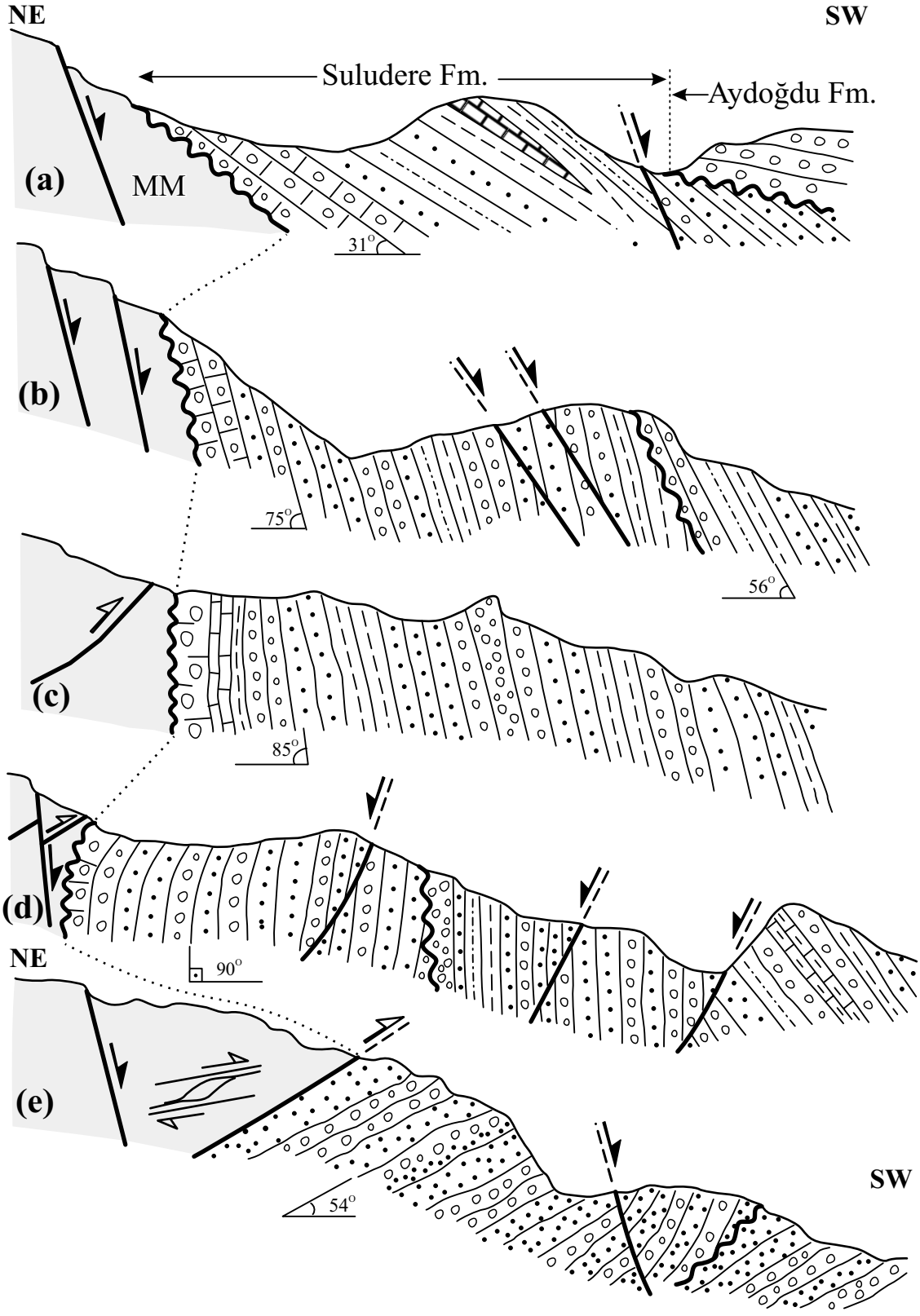
NE
SW
Suludere Fm.
Aydoğdu Fm.
(a)
MM
31°
(b)
75°
56°
(c)
85°
(d)
NE
90°
(e)
54°
SW

Figure 13. Representative field cross-sections taken from the northern margin of the Kiraz Basin. In all sections, note location of the Suludere Fault (high-angle normal fault) is very close to the main stratigraphic (unconformity) and structural (reverse fault) contact along the northern margin of the Kiraz Basin. **(a)** This cross-section shows a low-angle unconformable contact (average dip is 31°) between the Miocene sediments and the underlying metamorphic rocks of the Menderes Massif. Note the carbonate cemented conglomerate facies rests directly on the metamorphic rocks. Towards the south, Plio–Quaternary Aydoğdu Formation rests unconformably on the moderately dipping sediments of the Suludere Formation. **(b)** Cross-section showing steeply dipping (up to 80°) northern boundary of the basin. Note variation in dips of bedding within the Suludere Formation creates an intraformational unconformity. **(c)** Cross-section showing vertical unconformity upon which carbonate-cemented conglomerate and sandy limestone facies directly rested. Note steeply dipping strata exist far from the unconformity. **(d)** Cross-section showing vertical to overturned unconformity north of which a brittle fault with oblique-slip reverse movement is established within the metamorphic basement. Note presence of an intraformational unconformity and the younger normal faults resulted in gradual decrease in dips of bedding towards the south. **(e)** Cross-section showing relationships between metamorphic rocks of the Menderes Massif and the structurally underlying Miocene sediments. Note presence of overturned Miocene bedding with an average of 54° found directly under the reverse fault. Attention to the intraformational unconformity towards the south. Note the structural features in the hanging wall of the reverse fault indicate top-to-the-south reverse motion. See Figure 4 for location of the cross-sections and Figure 14 for explanation of the lithologies.

Deformation Phases

The *D_1 deformation* is observed north of Beydağ along the marble-schist contact. In this zone, marbles of the Menderes Massif have been thrust over schists; the well-developed shear band foliation within the schists indicate northward tectonic transport. Tectonic transport to the north was a product of a N–S compressional regime in the Menderes Massif; this event corresponds to a period of latest Palaeogene crustal thickening in western Anatolia and the burial and metamorphism of the Menderes Massif beneath the Lycian Nappes (e.g., Şengör & Yılmaz 1981; Şengör *et al.* 1984; Bozkurt & Park, 1994, 1997; Bozkurt 1996, 2007; Hetzel *et al.* 1998; Lips *et al.* 2001; Whitney & Bozkurt 2002).

The *D_2 deformation* occurs in narrow shear zones within the elevated schists to the south of Beydağ. Products of this deformation, shear band foliations are consistent with a top-to-the-south tectonic transport. In western Anatolia, the D_2 deformation is represented by the exhumation of the Menderes Massif in the footwall blocks of now low-angle shear zones and/or normal faults (Bozkurt & Park 1994), the formation of supradetachment basins (Emre & Sözbilir 1995; Emre 1996a, b; Sözbilir & Emre 1996; Koçyiğit *et al.* 1999; Bozkurt 2000; Gessner *et al.* 2001; Işık & Tekeli 2001; Lips *et al.* 2001; Sözbilir 2001, 2002; Seyitoğlu *et al.* 2000, 2002; Işık *et al.* 2003, 2004; Bozkurt & Sözbilir 2004; Purvis & Robertson 2004, 2005), and granitic intrusions which have developed in footwall blocks (e.g., Hetzel *et al.* 1995b; Bozkurt & Park 1994, 1997; Işık *et al.* 2003, 2004; Bozkurt 2004).

The *D_3 deformation* is represented by intrabasinal unconformities developed at the lower part of the Suludere Formation; strike-slip faults and reverse faults between metamorphic rocks of the Menderes Massif and the Suludere formation form the other conspicuous elements. This basin-forming synsedimentary tectonics is recorded for the first time in the present study. During this phase the basin was shaped as an asymmetric sedimentary trough closely associated with uplift of the northern margin. This trough was bounded to the east and west by the basement-involved NE-trending strike-slip systems. Slip along the NE-trending basement faults resulted in uplift of basement blocks, and led to shortening in overlap zones between the faults. This resulted in reverse slip along the boundary between the Menderes Massif and the structurally underlying Miocene sediments; and the formation of a push-up zone. The thrusting of Menderes Massif over the Miocene sediments indicates post-sedimentary compressional tectonics that recently have been recorded in several Miocene depression in western Anatolia (Koçyiğit *et al.* 1999; Kaya *et al.* 2004; Bozkurt & Rojay 2005; Bozkurt & Sözbilir 2006).

The *D_4 deformation* is observed along approximately NW–SE- and WNW–ESE-trending fault zones, such as the Suludere, Beydağ and Halıköy faults which controlled the formation of Kiraz depression. The D_4 deformation corresponds to the N–S- to NE–SW-oriented Plio–Quaternary extensional period developed in relation to high-angle normal faults. This phase of deformation in western Anatolia has been described from the Gediz (e.g., Emre 1996a, b; Sözbilir & Emre 1996; Koçyiğit *et al.* 1999; Sözbilir 2001, 2002; Bozkurt & Sözbilir 2004), Büyük Menderes (e.g., Emre & Sözbilir 1995; Sözbilir & Emre 1996; Bozkurt 2000, 2001b; Özer & Sözbilir 2003) and Küçük Menderes grabens (Bozkurt & Rojay 2005; Rojay *et al.* 2005). During this period, sediments of the Plio–Pleistocene Aydoğdu Formation were

deposited in alluvial fans – whose axes are oriented N–S and NE–SW – by very high-energy, rapid load-dumping streams. The collective activity of the high-angle normal faults associated with some strike-slip fault sets gives the study area its present morphological configuration. This deformation, the influence of which continues, shapes the plains that are filled with the youngest alluvium.

Recently, Bozkurt & Rojay (2005) defined four distinct phases of Alpine deformation (D_1–D_4) with respect to structural data collected from the northern part of the Kiraz Basin. These are: (1) Imbrication and crustal stacking of the Menderes Massif by the top-north contractional deformation (D_1) operated during the Eocene main Menderes metamorphism, (2) crustal thinning and consequent N–S-trending extensional exhumation of Menderes Massif by bivergent deformation (D_2) during the Oligo–Miocene, (3) post-Early Pliocene compressional tectonics that characterized by an oblique-slip reverse fault with a dextral component (D_3) resulted in emplacement of Menderes Massif onto the Neogene units, and (4) approximately E–W-trending graben-bounding high-angle normal faults (D_4) correspond to second phase extension in the Kiraz Basin. The four stages of deformation also show a good agreement with the work of Bozkurt & Rojay (2005), although in the present work, the formation of the oldest sedimentary package in the Kiraz Basin is attributed to contractional rather than extensional deformation.

Tectonic Evolution of the Kiraz Basin

During the first stage, at the end of the Middle Miocene, the region was under the control of compressional tectonics associated with uplift (Figure 14a). This resulted in a syncline-shaped depression that was covered by small lakes of only moderate depth, but with conditions suitable for algae and ostracodes to survive. These fresh-water coastal lakes were originally under the influence of surface streams that were connected to the open sea, but in later periods there was no marine contribution. Lake-shore carbonates of the Suludere formation developed in these lakes and unconformably overlie the volcanic rocks. Shallow-lake carbonates were followed upward by slightly meandering-river-channel and floodplain sediments (Emre *et al.* 2006). The sediments lying atop the limestones were deposited in a slightly sloping topography. The suddenly decrease in fine-clastics and increase in conglomerates and pebbly sandstones, suggest increases in the slope of the topography along the northern margin of the basin. The sudden changes in lithologies are also in accordance with sudden variation in dip of bedding. This is resulted in intraformatinal unconformities that were controlled by a synsedimentary asymmetric uplift and N–S compression during the late Middle Miocene–Late Miocene time (Figure 14b).

The N–S-trending compression-related basin formation ended when the metamorphic rocks of the Menderes Massif thrust over the Miocene basin sediments during the Early–Middle (?) Pliocene (Figure 14c). The angular unconformity between the Suludere and Aydoğdu formations marks this post-Late Miocene depositional hiatus that may correspond to a Early–Middle Pliocene compressional phase described from the Gediz Graben (Koçyiğit *et al.* 1999) and Küçük Menderes Graben (Bozkurt & Rojay 2005). The second stage of basin evolution is represented by block faulting that developed under the control of approximately N–S extensional tectonics (Figure 14d). Structural elements of this stage have been superimposed and masked on the former contractional structures (Figure 15). During this stage, alluvial fan sedimentation of the Plio–Quaternary age is formed in front of the high-angle normal faults.

Conclusion

1. In the Kiraz Basin, the 14.3±0.1–14.7±0.1 Ma Başova andesites and metamorphic rocks of the Menderes Massif form the basement for the basin. The basin fill units overlying unconformably the basement rocks, comprise the uppermost Middle Miocene–Upper Miocene Suludere Formation, the Plio–Pleistocene Aydoğdu Formation and Holocene alluvium;
2. In the study area, four phases of deformation (D_1–D_4) and three interrelated faults sets have been recognized. Following deformation phases D_1 and D_2, characterized by tectonic transport to the north and south, respectively, D_3 is attributed to a syn- to post-sedimentary compressional tectonics, D_4 as high-angle normal faulting. The D_1 deformation corresponds to a N–S regional contractional tectonic regime; D_2 to a N–S extensional tectonic regime that controlled the exhumation of the Menderes Massif in the footwall blocks of the now low-angle normal faults and the formation of supradetachment basins; D_3 to a late

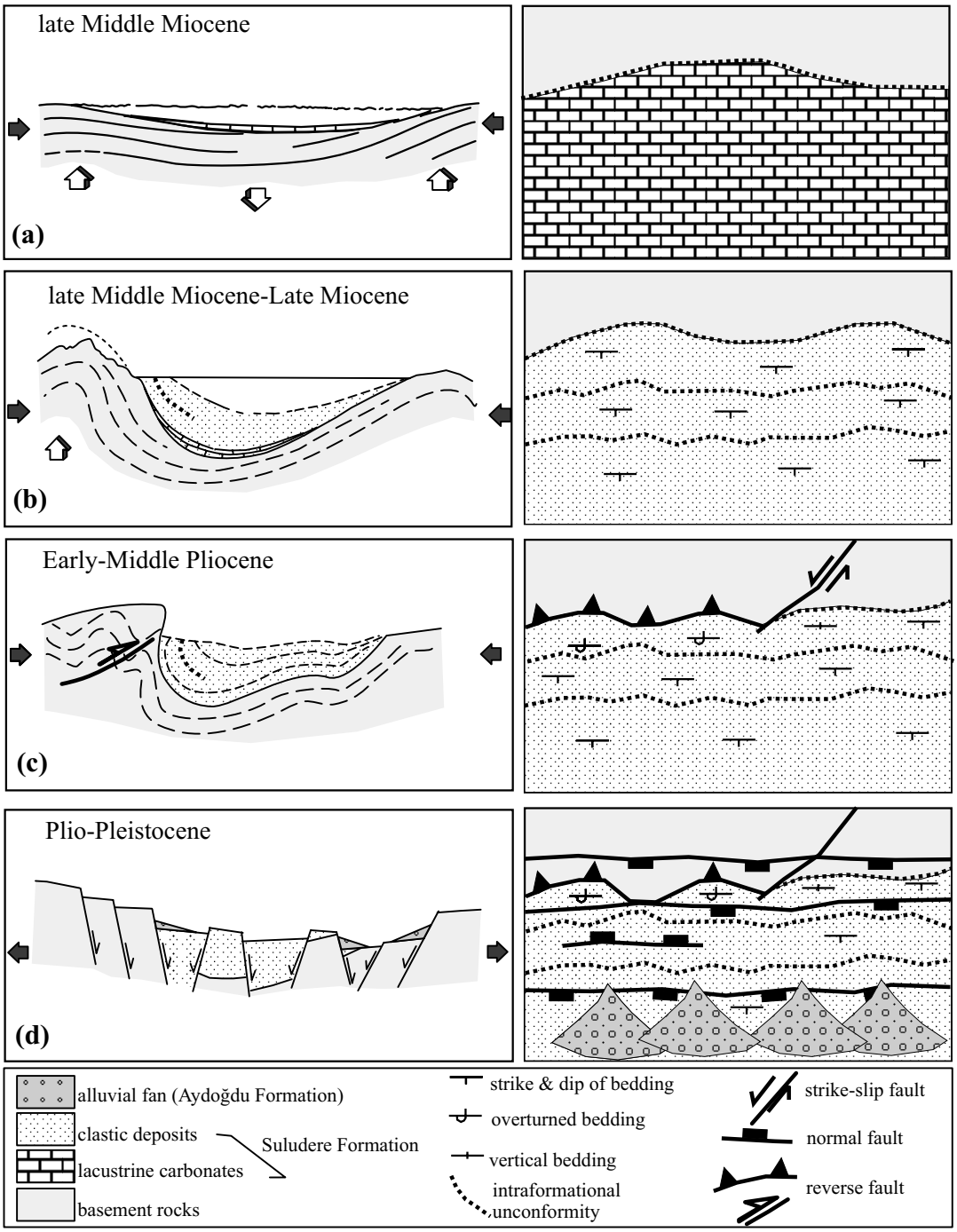

Figure 14. Schematic representation of the tectonic evolution of the Kiraz Basin. Note left column shows representative cross-sections in N–S directions, and right column indicative of the palaeocographic sketch maps of the northern margin of the basin during main phases of basin evolution. (a) Latest Middle Miocene: formation of small lakes under the control of compression associated with uplift. (b) Late Middle Miocene–Late Miocene: continuous uplift and N–S compression during sedimentation resulted in intraformational unconformities along the northern margin of the basin. (c) Early–Middle Pliocene: reverse faulting associated with strike-slip faults along the northern margin of the basin post-date sedimentation of the Suludere Formation. (d) Plio–Quaternary: block faulting developed under the control of N–S extensional tectonics that masked and overprinted on the earlier contractional structures. Formation of the alluvial fan sedimentation in front of the high-angle normal faults.

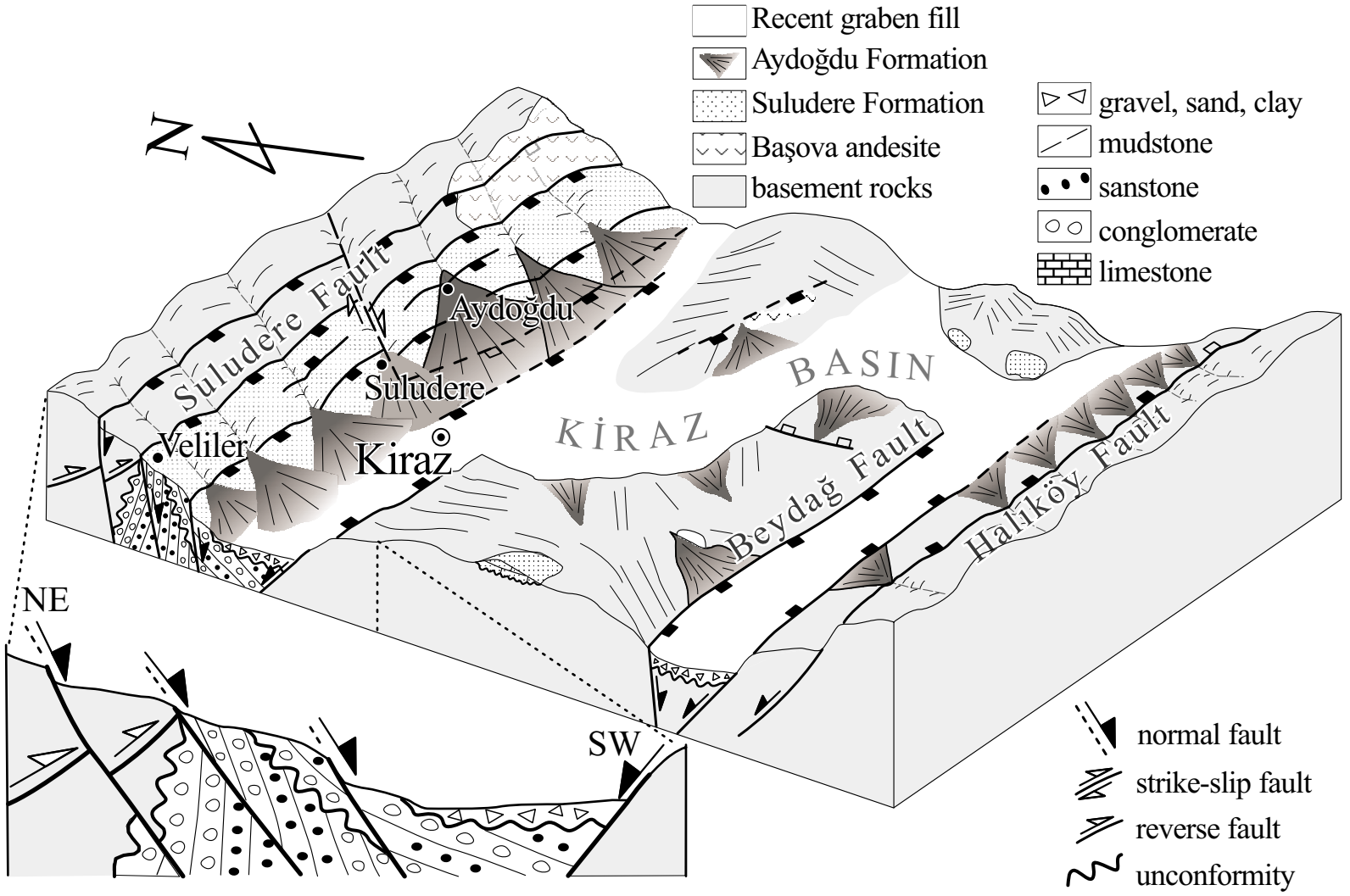

Figure 15. Block diagram depicting a tentative two stage episodic evolution of the Kiraz Basin. Note compression-related structures superposed by extensional high-angle normal faults. Attention to structural relationships among the Suludere Fault, reverse fault and the basal unconfornity in an exaggerated cross-section and to surface expression of the Suludere fault in the block diagram.

Middle Miocene–Middle Pliocene contractional tectonic regime; and the D_4 phase to a period of N–S- to NE–SW-oriented extension in the Plio–Quaternary during which high-angle normal faults developed.

3. The development of the oldest sedimentary package of the Kiraz Basin has been related to normal faulting, and interpreted as a half-graben with the master fault along its northern margin (Bozkurt & Rojay 2005). However, the structural setting of this basin suggests a more complex tectonic history, since the Suludere formation is affected by synsedimentary compressive deformation. The result of the detailed work also demonstrates the existence of intraformational unconformities in the northern margin of the basin. This new interpretation requires a revision of the existing regional approaches to the tectonic setting of the west Anatolian basins. The oldest basin fills have been affected by a NW-trending border fault associated with NE-trending strike-slip faults, and along this margin, clastic sediments are tilted strongly basinward, even slightly overturned beds have been observed. Between the strike-slip faults where noticeable horizontal slip was involved, sedimentation was strongly influenced by uplift. As a consequence, the horizontal slip on the basement faults resulted in basement upthrusts, and flexures with horizontal axes, which caused vertical movements to affect the northern basin margin. Thickness of the basin sediments shows a progressive southward decrease.
4. In addition to algae and ostracod fossils, lacustrine carbonate sediments at the base of the uppermost Middle Miocene–Upper Miocene Suludere Formation contain poorly preserved planktic and benthic foraminifera, showing that these lakes were initially under the influence of surface streams which connected to the open sea.
5. Following the Late Miocene, a depositional hiatus (reflected by the angular unconformity between the Suludere and Aydoğdu formations) and the thrusting of Menderes Massif rocks onto the Suludere Formation indicate that a contractional regime was active.
6. The development of the Plio–Pleistocene Aydoğdu Formation, under the control of the Suludere and Halıköy faults that bound the Kiraz Basin to the north and south, demonstrate that the extensional tectonic regime initiated the second stage sedimentation within the Kiraz Basin. This phase corresponds to a widening of the basin in N–S direction up to present.

Acknowledgements

This study was carried out within the framework of TÜBİTAK Project No. YDABAG-102Y052. The authors would like to express their special thanks to anonymous referees whose comments and criticisms have greatly improved the earlier version of the paper. Special thanks must go to Metin Tavlan and Bora Uzel for drawing the figures. Darrel Maddy helped with the English.

References

AKÇAY, M., ÖZKAN, H.M., MOON, C.J. & SPIRO, B. 2006. Geology, mineralogy and geochemistry of the gold-bearing stibnite and cinnibar deposits in the Emirli and Halıköy areas (Ödemiş, İzmir, West Turkey). *Ore Geology Reviews* **29**, 19–51.

ALDANMAZ, E. 2006. Mineral-chemical constraints on the Miocene calc-alkaline and shoshonitic volcanic rocks of Western Turkey: disequilibrium phenocryst assemblages as indicators of magma storage and mixing conditions. *Turkish Journal of Earth Sciences* **15**, 47–73.

ANGELIER, J. 1984. Tectonic analysis of fault slips data sets. *Journal of Geophysical Research* **80**, 5835–5848.

ANGELIER, J. 1991. Inversion of field data in fault tectonics to obtain regional stress III: a new rapid direct inversion method by analytical means. *Geophysical Journal International* **103**, 363–76.

ANGELIER, J. 1994. Fault slips analysis and paleostress reconstruction. *In*: Hancock, P.L. (ed), *Continental Deformation*. Pergamon Press, Oxford, 53–100.

ANGELIER, J., DUMONT, J.F., KARAMANDERESİ, İ.H., POISSON, A., ŞİMŞEK, Ş. & UYSAL, Ş. 1981. Analyses of fault mechanisms and expansion of southwestern Anatolia since the Late Miocene. *Tectonophysics* **79**, 11–19.

ARPAT, E. & BİNGÖL, E. 1969. Ege Bölgesi graben sisteminin gelişimi üzerine düşünceler [The rift system of western Turkey: thoughts on its developments]. *Mineral Research and Exploration Institute (MTA) of Turkey Bulletin* **73**, 1–9 [in Turkish with English abstract].

BOZKURT, E. 1996. Metamorphism of Palaeozoic schists in the southern Menderes Massif: field, petrographic, textural and microstructural evidence. *Turkish Journal of Earth Sciences* **5**, 105–121.

BOZKURT, E. 2000. Timing of extension on the Büyük Menderes Graben, Western Turkey and its tectonic implications. *In:* BOZKURT, E., WINCHESTER, J.A. & PIPER, J.D.A. (eds), *Tectonics and Magmatism in Turkey and the Surrounding Area*. Geological Society, London, Special Publications **173**, 385–403.

BOZKURT, E. 2001a. Late Alpine evolution of the central Menderes Massif, western Anatolia, Turkey. *International Journal of Earth Sciences* **89**, 728–744.

BOZKURT, E. 2001b. Neotectonics of Turkey – a synthesis. *Geodinamica Acta* **14**, 3–30.

BOZKURT, E. 2002. Discussion on the extensional folding in the Alaşehir (Gediz) Graben, western Turkey. *Journal of the Geological Society, London* **159**, 105–109.

BOZKURT, E. 2003. Origin of NE-trending basins in western Turkey. *Geodinamica Acta* **16**, 61–81.

BOZKURT, E. 2004. Granitoid rocks of the southern Menderes Massif (southwestern Turkey): field evidence for Tertiary magmatism in an extensional shear zone. *International Journal of Earth Sciences* **93**, 52–71.

BOZKURT, E. 2007. Extensional v. contractional origin for the southern Menderes shear zone, SW Turkey: tectonic and metamorphic implications. *Geological Magazine* **144**, 191–210.

BOZKURT, E. *&* OBERHÄNSLI, R. 2001. Menderes Massif (western Turkey): structural, metamorphic and magmatic evolution – a synthesis. *International Journal of Earth Sciences* **89**, 679–708.

BOZKURT, E. & PARK, R.G. 1994. Southern Menderes Massif: an incipient metamorphic core complex in western Anatolia, Turkey. *Journal of the Geological Society, London* **151**, 213–216.

BOZKURT, E. *&* PARK, R. 1997. Microstructures of deformed grains in the augen gneisses of southern Menderes massif (western Turkey) and their tectonic significance. *Geologische Rundschau* **86**, 103–119.

BOZKURT, E & ROJAY, B. 2005. Episodic, two-stage Neogene extension and short-term intervening compression in western Anatolia: field evidence from the Kiraz Basin and Bozdağ Horst. *Geodinamica Acta* **18**, 295–312.

BOZKURT, E. & SÖZBİLİR, H. 2004. Tectonic evolution of the Gediz Graben: field evidence for an episodic, two-stage extension in western Turkey. *Geological Magazine* **141**, 63–79.

BOZKURT, E. & SÖZBİLİR, H. 2006. Evolution of the large-scale active Manisa Fault, Southwest Turkey: implications on fault development and regional tectonics. *Geodinamica Acta* **19**, 427–453.

CANDAN, O., DORA, O.Ö., OBERHANSLI, R., ÇETİNKAPLAN, M., PARTZSCH, J.H., WARKUS, F.C. & DÜRR, S. 2001. Pan-African high-pressure metamorphism in the Precambrian basement of the Menderes Massif, western Anatolia, Turkey. *International Journal of Earth Sciences* **89**, 793–811.

ÇİFTÇİ, N.B. & BOZKURT, E. 2007. Anomalous stress field and active breaching at relay ramps: a field example from Gediz Graben, SW Turkey. *Geological Magazine* **144**, 687–699.

DEWEY, J.F. & ŞENGÖR, A.M.C. 1979. Aegean and surrounding regions: complex multiple and continuum tectonics in a convergent zone. *Geological Society of America Bulletin* **90**, 84–92.

DOGLIONI, C., AGOSTINI, S., CRESPI, M., INNOCENTI, F., MANETTI, P., RIGUZZI, F. & SAVAÇŞIN, M.Y. 2002. On the extension in Western Anatolia and the Aegean Sea. *Journal of Virtual Exploration* **8**, 169–183.

DUMONT, J.F., UYSAL, Ş., ŞİMŞEK, Ş., KARAMANDERESİ, İ.H. & LETOUZEY, J. 1979. Güneybatı Anadolu'daki grabenlerin oluşumu [Formation of West Anatolian grabens]. *Mineral Research and Exploration Institute (MTA) of Turkey Bulletin* **92**, 7–7 [in Turkish with English abstract].

EMRE, T. 1996a. Gediz Grabeni'nin jeolojisi ve tektoniği [Geology and tectonics of the Gediz Graben]. *Turkish Journal of Earth Sciences* **5**, 171–185 [in Turkish with English abstract].

EMRE, T. 1996b. Gediz Grabeni'nin tektonik evrimi [Tectonic evolution of the Gediz Graben]. *Geological Bulletin of Turkey* **39**, 1–18 [English edition].

EMRE, T. & SÖZBİLİR, H. 1995. Field evidence for metamorphic core complex, detachment faulting and accommodation faults in the Gediz and Büyük Menderes grabens, western Anatolia. *In:* PİŞKİN, Ö., ERGÜN, M., SAVAŞÇIN, M.Y. & TARCAN, G. (eds), *Proceedings of International Earth Science Colloquium on the Aegean Region* **1**, 73–93.

EMRE, T. & SÖZBİLİR, H. 2005. Geology, geochemistry and geochronology of the Başova andesite, eastern end of the Küçük Menderes Graben. *Mineral Research and Exploration Institute (MTA) of Turkey Bulletin* **131**, 1–19 [English edition].

EMRE,T., SÖZBİLİR, H. & GÖKÇEN, N. 2006. Neogene-Quternary stratigraphy of Kiraz-Beydağ region, Küçük Menderes Graben, West Anatolia. *Mineral Research and Exploration Institute (MTA) of Turkey Bulletin* **132**, 1–32 [in Turkish with English abstract].

ERİNÇ, S. 1955. Die morduologischen Entwicklungsstadien der Küçükmenderes Masse. *Rewiew of the Geographical Enstitute of the University of İstanbul* **2**, 93–95.

ERKÜL, F., HELVACI, C. & SÖZBİLİR, H. 2005a. Evidence for two episodes of volcanism in the Bigadiç borate basin and tectonic implications for western Turkey. *Geological Journal* **40**, 545–570.

ERKÜL, F., HELVACI, C. & SÖZBİLİR, H. 2005b. Stratigraphy and geochronology of the Early Miocene volcanic units in the Bigadiç borate basin, western Turkey. *Turkish Journal of Earth Sciences* **14**, 1–27.

ERKÜL, F., HELVACI, C. & SÖZBİLİR, H. 2006. Olivine basalt and trachandesite peperites formed at the subsurface/surface interface of a semi-arid lake: an example from the Early Miocene Bigadiç basin, western Turkey. *Journal of Volcanology and Geothermal Research* **149**, 240–262.

ERSOY, Y. & HELVACI, C. 2007. Stratigraphy and geochemical features of the Early Miocene Bimodal (ultrapotassic and calc-alkaline) volcanic activity within the NE-trending Selendi Basin, Western Anatolia, Turkey. *Turkish Journal of Earth Sciences* **16**, 117–139.

GESSNER, K., RING, U., CHRISTOPHER, J., HETZEL, R., PASSCHIER, C.W. & GÜNGÖR, T. 2001. An active bivergent rolling-hinge detachment system: central Menderes metamorphic core complex in western Turkey. *Geology* **29**, 611–614.

GLODNY, J. & HETZEL, R. 2007. Precise U–Pb ages of syn-extensional Miocene intrusions in the central Menderes Massif, western Turkey. *Geological Magazine* **144**, 235–246

GÖKTEN, E., HAVZAOĞULU, Ş. & ŞAN, Ö. 2001. Tertiary evolution of the central Menderes Massif based on structural investigations of metamorphics and sedimentary cover rocks between Salihli and Kiraz (western Turkey). *International Journal of Earth Sciences* **89**, 745–756.

GÖRÜR, N., ŞENGÖR, A.M.C., SAKINÇ, M., TÜYSÜZ, O., AKKÖK, R., YİĞİTBAŞ, E., OKTAY, F.Y., BARKA, A.A., SARICA, N., ECEVİTOĞLU, B., DEMİRBAĞ, E., ERSOY, Ş., ALGAN, O., GÜNEYSU, C. & AKYOL, A. 1995. Rift formation in the Gökova region, southwest Anatolia: implications for the opening of the Aegean Sea. *Geological Magazine* **132**, 637–650.

HETZEL, R., PASSCHIER, C.W., RING, U. & DORA, O.O. 1995a. Bivergent extension in orogenic belts: the Menderes Massif (southwestern Turkey). *Geology* **23**, 455–458.

HETZEL, R., RING, U., AKAL, C. & TROESCH, M. 1995b. Miocene NNE-directed extensional unroofing in the Menderes Massif, southwestern Turkey. *Journal of the Geological Society, London* **152**, 639–654.

HETZEL, R., ROMER, R.L., CANDAN, O. & PASSCHIER, C.W. 1998. Geology of the Bozdağ area, central Menderes Massif, SW Turkey: Pan-African basement and Alpine deformation. *Geologische Rundschau* **87**, 394–406.

IŞIK, V., SEYİTOĞLU, G. & ÇEMEN, İ. 2003. Ductile-brittle transition along the Alaşehir detachment fault and its structural relationship with the Simav detachment fault, Menderes Massif, western Turkey. *Tectonophysics* **374**, 1–18.

IŞIK, V. & TEKELİ, O. 2001. Late orogenic crustal extension in the northern Menderes Massif (western Turkey): evidence for metamorphic core complex formation. *International Journal of Earth Sciences* **89**, 757–765.

IŞIK, V., TEKELİ, O. & SEYİTOĞLU, G. 2004. The $^{40}Ar/^{39}Ar$ age of extensional ductile deformation and granitoid intrusion in the northern Menderes core complex: implications for the initiation of extensional tectonics in western Turkey. *Journal of Asian Earth Sciences* **23**, 555–566.

KAYA, O., ÜNAY, E., GÖKTAŞ F. & SARAÇ, G. 2007. Early Miocene stratigraphy of central West Anatolia, Turkey: implications for the tectonic evolution of the Eastern Aegean area. *Geological Journal* **42**, 85–109.

KAYA, O., ÜNAY, E., SARAÇ, G., EICHHORN, S., HASSENRUCK, S., KNAPPE, A., PEKDEĞER, A. & MAYDA, S. 2004. Halitpaşa transpressive zone: implications for an Early Pliocene compressional phase in central westen Anatolia, Turkey. *Turkish Journal of Earth Sciences* **13**, 1–13.

KOÇYİĞİT, A. 1984. Güneybatı Türkiye ve yakın dolayında levha içi yeni tektonik gelişim [Intraplate neotectonic evolution of the southwest Turkey and its surroundings]. *Geological Society of Turkey Bulletin* **27**, 1–16 [in Turkish with English abstract].

KOÇYİĞİT, A., YUSUFOĞLU, H. & BOZKURT, E. 1999. Evidence from the Gediz graben for episodic two-stage extension in western Turkey. *Journal of the Geological Society, London* **156**, 605–616.

LE PICHON, X. & ANGELIER, J. 1979. The Aegean arc and trench system: a key to the neotectonic evolution of the eastern Mediterranean area. *Tectonophysics* **60**, 1–42.

LE PICHON, X. & ANGELIER. J. 1981. The Agean sea. *Philosophical Transactions of Royal Society, London* **300**, 357–372.

LIPS, A.L.W., CASSARD, D., SÖZBİLİR, H., YILMAZ, H. & WIJBRANS, J. 2001. Multistage exhumation of the Menderes Massif, western Anatolia (Turkey). *International Journal of Earth Sciences* **89**, 781–792.

MCKENZIE, D.P. 1972. Active tectonics of the Mediterranean regions, *Geophysical Journal of Royal Astronomical Society* **30**, 109–185.

OKAY, A.İ. & SATIR, M. 2000. Coeval plutonism and metamorphism in a latest Oligocene metamorphic core complex in northwest Turkey. *Geological Magazine* **137**, 495–516.

ÖZER, S. & SÖZBİLİR, H. 2003. Presence and tectonic significance of Cretaceous rudist species in the so-called Permo–Carboniferous Göktepe Formation, Central Menderes Metamorphic Massif, Western Turkey. *International Journal of Earth Sciences* **92**, 397–404.

PURVIS, M. & ROBERTSON, A. 2004. A pulsed extension model for the Neogene–Recent E–W-trending Alaşehir Graben and the NE–SW-trending Selendi and Gördes basins, western Turkey. *Tectonophysics* **391**, 171–201.

PURVIS, M. & ROBERTSON, A. 2005. Sedimentation of the Neogene–Recent Alaşehir (Gediz) continental graben system used to test alternative tectonic models for western (Aegean) Turkey. *Sedimentary Geology* **173**, 373–408.

RIBA, O. 1976. Syntectonic unconformities of the Alto Cardener, Spanish Pyrenees: a genetic interpretation. *Sedimentary Geology* **15**, 213–233.

RING, U., GESSNER, K., GÜNGÖR, T. & PASSCHIER, C.W. 1999. The Menderes belt of western Turkey and the Cycladic belt in the Aegean – do they really correlate? *Journal of the Geological Society, London* **156**, 3–6.

ROJAY, B., TOPRAK, V., DEMİRCİ, C. & SÜZEN, L. 2005. Plio–Quaternary evolution of the Küçük Menderes Graben Southwestern Anatolia, Turkey. *Geodinamica Acta* **18**, 317–331.

SARICA, N. 2000. The Plio–Pleistocene age of Büyük Menderes and Gediz grabens and their tectonic significance on N–S extensional tectonics in west Anatolia: mammalian evidence from the continental deposits. *Geological Journal* **35**, 1–24.

ŞENGÖR, A.M.C. 1979. The North Anatolian Transform Fault: its age, offset and tectonic significance. *Journal of the Geological Society, London* **136**, 269–282.

ŞENGÖR, A.M.C. 1987. Cross-faults and differential stretching of hanging walls in regions of low-angle normal faulting: examples from western Turkey. *In*: COWARD, M.P., DEWEY, J.F. & HANCOCK, P.L. (eds), *Continental Extensional Tectonics*. Geological Society, London, Special Publications **28**, 575–589.

ŞENGÖR, A.M.C., GÖRÜR, N. & ŞAROĞLU, F. 1985. Strike-slip faulting and related basin formation in zones of tectonic escape: Turkey as a case study. *In*: BIDDLE, K. & CHRISTIE-BLICK, N. (eds), *Strike-slip Deformation, Basin Formation and Sedimentation*. Society of Economic Paleontologists and Mineralogists, Special Publications **37**, 227–264.

ŞENGÖR, A.M.C., SATIR, M. & AKKÖK, R. 1984. Timing of tectonic events in the Menderes Massif, western Turkey: Implications for tectonic evolution and evidence for Pan-African basement in Turkey. *Tectonics* **3**, 693–707.

ŞENGÖR, A.M.C. & YILMAZ, Y. 1981. Tethyan evolution of Turkey: A plate tectonic approach. *Tectonophysics* **75**, 181–241.

ŞENGÜN, F., CANDAN, O., DORA, O.Ö. & KORALAY, E. 2006. Petrography and Geochemistry of Paragneisses in the Çine Submassif of the Menderes Massif, Western Anatolia. *Turkish Journal of Earth Sciences* **15**, 321–342.

SEYİTOĞLU, G., ÇEMEN, İ. & TEKELİ, O. 2000. Extensional folding in the Alaşehir (Gediz) Graben, western Turkey. *Journal of the Geological Society, London* **157**, 1097–1100.

SEYİTOĞLU, G., TEKELİ, O., ÇEMEN, İ., ŞEN, Ş. & IŞIK, V. 2002. The role of the flexural rotation/rolling hinge model in the tectonic evolution of the Alaşehir graben, western Turkey. *Geological Magazine* **139**, 15–26.

SEYİTOĞLU, G. & SCOTT, B.C. 1991. Late Cenozoic crustal extension and basin formation in west Turkey. *Geological Magazine* **128**, 155–166.

SEYİTOĞLU, G. & SCOTT, B.C. 1992. The age of the Büyük Menderes Graben (west Turkey) and its tectonic implications. *Geological Magazine* **129**, 239–242.

SEYİTOĞLU, G. & SCOTT, B.C. 1996. The age of the Alaşehir graben (west Turkey) and its tectonic implications. *Geological Journal* **31**, 1–11.

SEYİTOĞLU, G., SCOTT, B.C. & RUNDLE, C.C. 1992. Timing of Cenozoic extensional tectonics in west Turkey. *Journal of the Geological Society, London* **149**, 533–538.

SÖZBİLİR, H. 2001. Extensional tectonics and geometry of related macroscopic structures: field evidence from the Gediz detachment, Western Turkey. *Turkish Journal of Earth Sciences* **10**, 51–67.

SÖZBİLİR, H. 2002. Geometry and origin of folding in the Neogene sediments of the Gediz Graben, western Anatolia, Turkey. *Geodinamica Acta* **15**, 277–288.

SÖZBİLİR, H. 2005. Oligo–Miocene extension in the Lycian Orogen: evidence from the Lycian molasse basin, SW Turkey. *Geodinamica Acta* **18**, 255–282.

SÖZBİLİR, H. & EMRE, T. 1990. Neogene stratigraphy and structure of the northern rim of the Büyük Menderes graben. *In:* SAVAŞÇIN M.Y. & ERONAT, A.H. (eds), *Proceedings of International Earth Science Colloquium on the Aegean* Region **2**, 314–322.

SÖZBİLİR, H. & EMRE, T. 1996. Supradetachment basin and rift basin developed during the neotectonic evolution of the Menderes Massif. *Geological Congress of Turkey*, *Ankara, Abstracts*, 300–301.

TEMİZ, H., GÜRSOY, H. & TATAR, O. 1998. Kinematics of Late Pliocene–Quaternary normal faulting in the south-eastern end of the Gediz Graben, western Anatolia, Turkey. *International Geology Review* **40**, 638–646.

TOKCAER, M., AGOSTINI, S. & SAVAŞÇIN, M.Y. 2005. Geotectonic setting and origin of the youngest Kula volcanics (Western Anatolia), with a new emplacement model. *Turkish Journal of Earth Sciences* **14**, 143–166.

WHITNEY, D.L. & BOZKURT, E. 2002. Metamorphic history of the southern Menderes Massif, western Turkey. *Geological Society of America Bulletin* **114**, 829–838.

YILDIZ, M. & BAILEY, E.H. 1987. Mercury deposits in Turkey. *U.S. Geological Survey Bulletin* **1456**, 1–80.

YILMAZ, Y., GENÇ, S.C., GÜRER, O.F., BOZCU, M., YILMAZ, K., KARACIK, Z., ALTUNKAYNAK, Ş. & ELMAS, A. 2000. When did the western Anatolian grabens begin to develop? *In*: BOZKURT, E., WINCHESTER, J.A. & PIPER, J.D.A. (eds), *Tectonics and Magmatism in Turkey and the Surrounding Area*. Geological Society, London, Special Publications **173**, 353–384.

Received 14 August 2006; revised typescript received 01 March 2007; accepted 25 April 2007